SIAM J. APPL. MATH.
Vol. 75, No. 1, pp. 136–163

THE INTEGRABLE NATURE OF MODULATIONAL INSTABILITY*

GINO BIONDINI† AND EMILY FAGERSTROM†

Abstract. We investigate the nonlinear stage of the modulational (or Benjamin–Feir) instability by characterizing the initial value problem for the focusing nonlinear Schrödinger (NLS) equation with nonzero boundary conditions (NZBC) at infinity. We do so using the recently formulated inverse scattering transform (IST) for this problem. While the linearization of the NLS equation ceases to be valid when the perturbations have grown sufficiently large compared to the background, the results of the IST remain valid for all times and therefore provide a convenient way to study the nonlinear stage of the modulational instability. We begin by studying the spectral problem for the Dirac operator (i.e., the first half of the Lax pair for the NLS equation) with piecewise constant initial conditions which are a generalization to NZBC of a potential well and a potential barrier. Since the scattering data uniquely determine the time evolution of the initial condition via the inverse problem, the study of these kinds of potentials provides a simple means of investigating the growth of small perturbations of a constant background via IST. We obtain several results. First, we prove that there are arbitrarily small perturbations of the constant background for which there are discrete eigenvalues, which shows that no area theorem is possible for the NLS equation with NZBC. Second, we prove that there is a class of perturbations for which no discrete eigenvalues are present. In particular, this latter result shows that solitons cannot be the primary vehicle for the manifestation of the instability, contrary to a recent conjecture. We supplement these results with a numerical study about the existence, number, and location of discrete eigenvalues in other situations. Finally, we compute the small-deviation limit of the IST, and we compare it with the direct linearization of the NLS equation around a constant background, which allows us to precisely identify the nonlinear analogue of the unstable Fourier modes within the IST. These are the Jost eigenfunctions for values of the scattering parameter belonging to a finite interval of the imaginary axis around the origin. Importantly, this last result shows that the IST contains an automatic mechanism for the saturation of the modulational instability.

Key words. modulational instability, Benjamin–Feir instability, nonlinear Schrödinger equation, inverse scattering transform, nonzero boundary conditions

AMS subject classifications. 35Q55, 37K15, 37K40, 37K45, 34L25, 34L40, 74J25, 74J30

DOI. 10.1137/140965089

1. Introduction.

Modulational instability (MI)—i.e., the instability of a constant background with respect to long wavelength perturbations—is one of the most ubiquitous types of instability in nature. It arises in deep water waves, where it is known as the Benjamin–Feir instability [8, 7] (e.g., see [16] and references therein). It also appears in a variety of other physical settings such as nonlinear optics, plasmas, and Bose–Einstein condensates (see [6, 29, 34, 40, 41], as well as [50] for an overview and a historical review of the subject).

In many cases, the dynamics for a system exhibiting MI is governed to leading order by the focusing [$\nu = -1$] nonlinear Schrödinger (NLS) equation [6, 29, 34], namely,

$$iq_t + q_{xx} - 2\nu|q|^2 q = 0\,, \tag{1.1}$$

where $\nu = 1$ denotes the defocusing case, and where the physical meaning of the coordinates (x, t) depends on the context. For example, in water waves $q(x, t)$ is the

*Received by the editors April 15, 2014; accepted for publication (in revised form) October 29, 2014; published electronically January 27, 2015. This work was supported in part by the National Science Foundation under grant DMS-1311847.
http://www.siam.org/journals/siap/75-1/96508.html
†Department of Mathematics, State University of New York, Buffalo, NY 14260 (biondini@buffalo.edu, emilyrf@buffalo.edu).

complex envelope of the wave elevation from the undisturbed level, while in optical fibers $q(x,t)$ is the complex envelope of the electromagnetic field. In both settings, the NLS equation applies in a reference frame that moves with the group velocity of the carrier wave. (In optics, however, x represents the retarded time and t the physical propagation distance.)

Since (1.1) governs the modulations of a quasi-monochromatic wave packet, one can use it to study the stability properties of a uniform wave train. The solution $q_a(x,t) = a\,\mathrm{e}^{-2i\nu a^2 t}$ (where without loss of generality a is taken to be real and positive) is uniform and stationary in the xt-frame of coordinates, but in those physical contexts in which the NLS equation is an envelope equation, it describes a plane wave. For example, in water waves such a solution is the leading-order approximation of the Stokes wave, whereas in nonlinear optics it describes a continuous wave [29, 34, 47].

A linear stability analysis around the background solution $q_a(x,t)$ shows that it is stable in the defocusing case, but it is unstable to long wavelength perturbations in the focusing case. In optics, both the focusing and defocusing cases are possible depending on the material, the waveguide (slab or fiber, design, index profile, etc.), and the carrier wavelength. In water waves, however, only one case arises. The linearization ceases to be valid as soon as the perturbations have grown to the point that they are of comparable size compared to the background. A natural question is what happens at that point, which is referred to as the nonlinear stage of the modulational (Benjamin–Feir) instability. This question has remained open for almost 50 years.

Of course the NLS equation is also a completely integrable system. The infinite number of conserved quantities suggests that its solutions cannot blow up, and therefore that the growth of perturbations must remain bounded. The initial value problem (IVP) for (1.1) with initial conditions (IC) decaying as $x \to \pm\infty$ was solved by Zakharov and Shabat in 1972 [51] by developing an appropriate inverse scattering transform (IST) (see also [6, 21, 40, 41]). The background solution $q_a(x,t)$, however, satisfies nonzero boundary conditions (NZBC) as $x \to \pm\infty$ and is therefore outside the class of IC to which the above IST can be applied. Zakharov and Shabat also developed the IST for the defocusing NLS with NZBC [52] (see also [13, 21]). However, the IST for the *focusing* NLS equation with NZBC remained essentially an open problem until recently. We suspect that the reason for this oversight is that, since the constant background is unstable due to MI, one might be led to mistakenly conclude that such an IST would not be useful. However, MI is not an obstacle to IST. In fact, IST provides the *only* effective means of studying the nonlinear stage of MI! While a few IST-based studies of MI have been done for periodic boundary conditions [24, 30, 46], to the best of our knowledge no equivalent studies exist on the infinite line with NZBC.

The IST for the focusing NLS equation with NZBC was developed in [12]. Its availability makes it possible to investigate a variety of issues. Here we use it to perform an analytical study of the nonlinear stage of MI. Note that the focusing NLS equation with NZBC possesses a rich family of soliton solutions [44, 49]. Such solutions, all of which are nonstationary, reduce under certain limits to subfamilies found over the years by Kuznetsov and Ma (see [36, 38]), Peregrine [42], and Akhmediev (see [33]). In [49], using the dressing method, Zakharov and Gelash constructed a class of two-soliton solutions corresponding to small initial perturbations of a constant background, and they conjectured that the nonlinear stage of the MI is mediated by such soliton pairs. Here we will show that in many cases solitons do contribute to the over-

all solution of the problem. This is because there exists a class of perturbations of the constant background that generate a nontrivial discrete spectrum. On the other hand, we will also show that there exists another class of perturbations for which no discrete spectrum is present. Since *all* long-wavelength perturbations are linearly unstable, solitons *cannot* be the primary mechanism that describes the nonlinear stage of the MI.

Instead, we will show that the key to understanding the nonlinear stage of the MI is the contribution from the continuous spectrum in the IST. Usually, for IVPs that can be solved via IST, the radiative components of the solution (i.e., the contributions coming from the reflection coefficient) remain bounded in time, and in fact they vanish in the L^1 norm as $t \to \infty$. For example, this is the case for most nonlinear partial differential equations (PDEs) with zero boundary conditions (ZBC) at infinity, as well as for the defocusing NLS equation with NZBC [6, 21, 41]. For the *focusing* NLS equation with NZBC, in contrast, there exists a portion of the continuous spectrum (which is the set of values of the spectral parameter for which bounded eigenfunctions exist for the scattering problem) for which the simultaneous eigenfunctions of the Lax pair grow exponentially in time. Indeed, by taking the limit of the IST when the solution is a small deviation of the constant background, we will show that the leading-order term of the solution in this limit coincides exactly with the direct solution of the linearized NLS equation around the constant background. This shows that the regularization of the MI when the perturbations become sufficiently large is automatically built into the IST formalism. The situation is similar to what happens for Maxwell–Bloch systems of equations [1, 25, 26, 27, 31, 48], where the reflection coefficients can grow exponentially depending on the choice of boundary conditions. Just like in the Maxwell–Bloch case, however, the IST provides a mechanism that describes the automatic saturation of the instability.

The outline of this work is the following. In section 2, a brief review of the IST for the focusing NLS equation with NZBC is given, and the one-soliton solutions are discussed in section 3. In section 4, a specific class of piecewise-constant IC is considered which includes small perturbations of the constant background, and the associated spectral data are explicitly calculated. A characterization of the discrete spectrum for such piecewise-constant potentials is given in section 5, which will allow us to draw several general conclusions about the properties of the focusing NLS equation with NZBC. In section 6 we obtain the small-deviation limit of the IST, and we compare it to the linearization of the NLS equation around a constant background, which allows us to precisely identify the nonlinear analogue of the unstable Fourier modes. Section 7 concludes the work with a discussion of the results. Notation, proofs, and a few other technical results are contained in the appendices.

2. Inverse scattering transform for the focusing NLS equation with NZBC. Here we summarize the IST for the IVP for the focusing NLS equation (2.1) with the boundary conditions (2.2). We refer the reader to [12] for all details. We rewrite the focusing NLS equation as

$$iq_t + q_{xx} - 2\nu\,(|q|^2 - q_o^2)q = 0\,, \tag{2.1}$$

with the NZBC

$$\lim_{x\to\pm\infty} q(x,t) = q_\pm\,, \tag{2.2}$$

with $|q_\pm| = q_o \neq 0$. The rescaling $\tilde{q}(x,t) = q(x,t)\,\exp[-2i\nu q_o^2 t]$ yields (2.1) from (1.1), and is done so that the boundary values $q_\pm$ in (2.2) are independent of time. This

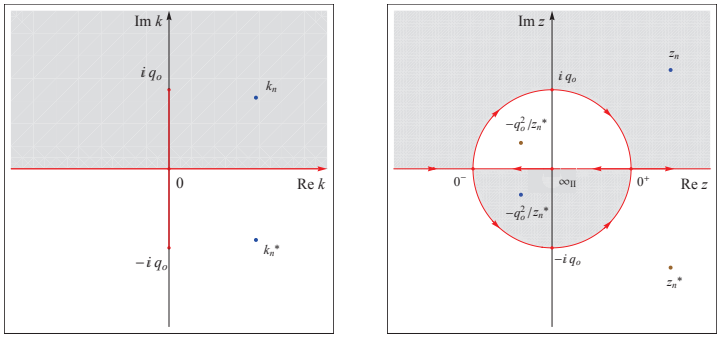

FIG. 1. *Left: The first sheet of the Riemann surface of the complex k-plane, showing the branch cut (segment $[-iq_o, iq_o]$ of the imaginary axis, in red online) and the region where $\operatorname{Im}\lambda > 0$ (gray). Right: The complex plane of the uniformization variable z. Shown in both cases are the regions $D^{\pm}$ (respectively in gray and white) where $\operatorname{Im}\lambda(z) \gtrless 0$. The oriented contours for the Riemann–Hilbert problem in the complex z-plane (see section 2.2) are also shown (in red online).*

simplifies the IST machinery. We dropped tildes for brevity, and hereafter we take $\nu = -1$.

Recall that (2.1) is the compatibility condition of the Lax pair

$$\phi_x = (ik\sigma_3 + Q)\,\phi\,, \qquad \phi_t = (-2ik^2\sigma_3 + H)\,\phi\,, \tag{2.3}$$

where $\phi(x,t,k)$ is a 2×2 matrix eigenfunction, σ_3 is the third Pauli matrix (A.1), and

$$Q(x,t) = \begin{pmatrix} 0 & q \\ -q^* & 0 \end{pmatrix}, \qquad H(x,t,k) = i\sigma_3(Q_x - Q^2 - q_o^2) - 2kQ\,.$$

The first equation of (2.3) is the scattering problem, $Q(x,t)$ is the scattering potential, and k is the scattering parameter.

2.1. Direct problem. As $x \to \pm\infty$, the solutions of the scattering problem are approximated by those of the asymptotic scattering problem $\phi_x = X_{\pm}\,\phi$, where $X_{\pm} = ik\sigma_3 + Q_{\pm}$ and $Q_{\pm} = \lim_{x\to\pm\infty} Q(x,t)$. The eigenvalues of $X_{\pm}$ are $\pm i\lambda$, where

$$\lambda(k) = (q_o^2 + k^2)^{1/2}\,. \tag{2.4}$$

We introduce the two-sheeted Riemann surface defined by $\lambda(k)$, taking the branch cut along the segment $i[-q_o, q_o]$. We also introduce the uniformization variable $z = k + \lambda$, which maps the two sheets of the complex k-plane, respectively, into the exterior and interior of the circle C_o of radius q_o centered at the origin in the complex z-plane. The inverse transformation is

$$k = (z - q_o^2/z)/2, \qquad \lambda = (z + q_o^2/z)/2\,. \tag{2.5}$$

With some abuse of notation we rewrite the k dependence as dependence on z. Note that $\operatorname{Im}(z)\,\lambda \gtrless 0$ in $D^{\pm}$, respectively, with $D^{\pm} = \{z \in \mathbb{C} : (\operatorname{Im} z)(|z|^2 - q_o^2) \gtrless 0\}$ (see Figure 1).

We write the eigenvector matrix for $X_{\pm}$ as $Y_{\pm}(z) = I + (i/z)\sigma_3 Q_{\pm}$, so that $X_{\pm}Y_{\pm} = Y_{\pm}\, i\lambda\sigma_3$. The continuous spectrum is $\Sigma_k = \mathbb{R} \cup i[-q_o, q_o]$, corresponding to $\Sigma_z = \mathbb{R} \cup C_o$ in the z-plane. Hereafter we omit the subscript on Σ, as the

intended meaning will be clear from the context. As $x \to \pm\infty$, the time evolution of the eigenfunctions is asymptotic to that of the solutions of $\phi_t = T_\pm \phi$, with $T_\pm = -2ik^2\sigma_3 - 2kQ_\pm$. Note that $T_\pm = -2kX_\pm$. Thus for all $z \in \Sigma$, we can define the Jost eigenfunctions $\phi_\pm(x,t,z)$ as the simultaneous solutions of both parts of the Lax pair satisfying the boundary conditions

$$\phi_\pm(x,t,z) = Y_\pm(z)\,\mathrm{e}^{i\theta(x,t,z)\sigma_3} + o(1) \qquad \text{as } x \to \pm\infty\,, \tag{2.6}$$

where $\theta(x,t,z) = \lambda(z)(x - 2k(z)t)$. An analysis of the Neumann series for the linear Volterra integral equations for the Jost eigenfunctions shows that their columns can be analytically extended to the following regions: $\phi_{+,1}$ and $\phi_{-,2}$ to $z \in D^+$, and $\phi_{-,1}$ and $\phi_{+,2}$ to $z \in D^-$. Hereafter, the additional subscripts 1 and 2 identify the matrix columns, i.e., $\phi_\pm(x,z,t) = (\phi_{\pm,1}, \phi_{\pm,2})$. Throughout this work, we use the *subscripts* $\pm$ to denote limiting values as $x \to \pm\infty$, and the *superscripts* $\pm$ to denote analyticity in the regions $D^\pm$.

For all $k \in \Sigma \setminus \{\pm iq_o\}$ and all $(x,t) \in \mathbb{R}^2$, one has $\det \phi_\pm(x,t,z) = 1 + q_o^2/z^2 \neq 0$. Hence, we can introduce a scattering matrix $S(z)$ as

$$\phi_+(x,t,z) = \phi_-(x,t,z)\,S(z)\,, \qquad z \in \Sigma\,. \tag{2.7}$$

Note that $S(z) = (s_{i,j})$ is independent of time. Also, $s_{1,1}(z)$ and $s_{2,2}(z)$ are analytic in D^+ and D^-, respectively, whereas $s_{1,2}(z)$ and $s_{2,1}(z)$ are nowhere analytic in general. The reflection coefficients needed in the inverse problem are

$$\rho(z) = s_{2,1}/s_{1,1}\,, \qquad \tilde\rho(z) = s_{1,2}/s_{2,2}\,, \qquad z \in \Sigma\,.$$

The scattering problem admits two symmetries: for all $z \in \Sigma$,

$$\phi_\pm(x,t,z) = \sigma_2 \phi_\pm^*(x,t,z^*)\sigma_2\,, \qquad \phi_\pm(x,t,z) = (i/z)\,\phi_\pm(x,t,-q_o^2/z)\,\sigma_3 Q_\pm\,.$$

These imply the following relations between the scattering coefficients:

$$\begin{aligned} s_{2,2}(z) &= s_{1,1}^*(z^*)\,, \qquad & s_{1,2}(z) &= -s_{2,1}^*(z^*)\,, \\ s_{1,1}(z) &= (q_+^*/q_-^*)\,s_{2,2}(-q_o^2/z)\,, \qquad & s_{1,2}(z) &= (q_+/q_-^*)\,s_{2,1}(-q_o^2/z)\,. \end{aligned}$$

In turn, these relations yield the symmetries for the reflection coefficients:

$$\rho(z) = -\tilde\rho^*(z^*) = (q_-/q_-^*)\,\tilde\rho(-q_o^2/z) = -(q_-^*/q_-)\,\rho^*(-q_o^2/z^*) \qquad \forall z \in \Sigma\,.$$

The discrete spectrum of the scattering problem comprises the zeros of $s_{1,1}(z)$ in D^+ and those of $s_{2,2}(z)$ in D^-. We ignore the possibility of zeros along Σ. If $s_{1,1}(z) = 0$ at $z = z_n$, the eigenfunctions $\phi_{+,1}$ and $\phi_{-,2}$ at $z = z_n$ must be proportional:

$$\phi_{+,1}(x,t,z_n) = b_n\,\phi_{-,2}(x,t,z_n)\,. \tag{2.8}$$

We assume that $s_{1,1}(z)$ has a finite number N of simple zeros $z_1, \ldots, z_N$ in D^+. The discrete spectrum is then the set $\{z_n, z_n^*, -q_o^2/z_n, -q_o^2/z_n^*\}_{n=1}^N$. Moreover, (2.8) implies

$$\begin{aligned} \mathrm{Res}_{z=z_n}\left[\phi_{+,1}(x,t,z)/s_{1,1}(z)\right] &= C_n\,\phi_{-,2}(x,t,z_n)\,, \quad & C_n &= b_n/s_{1,1}'(z_n)\,, \\ \mathrm{Res}_{z=z_n^*}\left[\phi_{+,2}(x,t,z)/s_{2,2}(z)\right] &= \tilde C_n\,\phi_{-,1}(x,t,z_n^*)\,, \quad & \tilde C_n &= \tilde b_n/s_{2,2}'(z_n^*)\,. \end{aligned}$$

From the symmetries, we have $\tilde{C}_n = -C_n^*$. Moreover,

$$\begin{aligned}\mathrm{Res}_{z=-q_o^2/z_n^*}\left[\phi_{+,1}(x,t,z)/s_{1,1}(z)\right] &= C_{N+n}\,\phi_{-,2}(x,t,-q_o^2/z_n^*)\,,\\ \mathrm{Res}_{z=-q_o^2/z_n}\left[\phi_{+,2}(x,t,z)/s_{2,2}(z)\right] &= \tilde{C}_{N+n}\,\phi_{-,1}(x,t,-q_o^2/z_n)\,,\end{aligned}$$

where $C_{N+n} = (q_o/z_n^*)^2(q_-^*/q_-)\,\tilde{C}_n$ and $\tilde{C}_{N+n} = (q_o/z_n)^2(q_-/q_-^*)\,C_n$.

Next we discuss the asymptotic behavior of the eigenfunctions and scattering coefficients as $k \to \infty$, which corresponds to $z \to \infty$ in $\mathbb{C}_{\mathrm{I}}$ and to $z \to 0$ in $\mathbb{C}_{\mathrm{II}}$. Considering the appropriate region of the complex plane for each column, one can show that $\phi_\pm(x,t,z) = \mathrm{e}^{i\theta(x,t,z)\sigma_3}(I + O(1/z))$ as $z \to \infty$. In particular, the asymptotic behavior of $\phi_-(x,t,z)$ will allow us to reconstruct the potential from the solution of the inverse problem in section 2.2:

$$\begin{aligned}\phi_-(x,t,z)\,\mathrm{e}^{i\theta(x,t,z)\sigma_3} &= I + (i/z)\sigma_3 Q(x,t)\\ &\quad + (i/z)\int_{-\infty}^{x}\big([\sigma_3 Q_-, \Delta Q_-(y,t)] + \Delta Q_-(y,t)\sigma_3\Delta Q_-(y,t)\big)\,\mathrm{d}y + O(1/z^2)\end{aligned} \tag{2.9}$$

as $z \to \infty$, where $\Delta Q_\pm(x,t) = Q(x,t) - Q_\pm$. Also, as $z \to \infty$ in the appropriate regions of the complex z-plane, $S(z) = I + O(1/z)$. Similarly, as $z \to 0$ in the appropriate regions of the z-plane, we have $\phi_\pm(x,t,z) = \mathrm{e}^{i\theta(x,t,z)\sigma_3}(i\sigma_3 Q_\pm/z + O(1))$ and $S(z) = \mathrm{diag}(q_-/q_+, q_+/q_-) + O(z)$.

2.2. Inverse problem. The inverse problem is formulated in terms of a matrix Riemann–Hilbert problem. The starting point is the scattering relation (2.7). We introduce modified eigenfunctions $\mu_\pm(x,t,z) = \phi_\pm(x,t,z)\,\mathrm{e}^{-i\theta(x,t,z)\sigma_3}$, which satisfy constant boundary conditions: $\mu_\pm(x,t,z) \to I$ as $x \to \pm\infty$. The analyticity properties of their columns are inherited from those of $\phi_\pm(x,t,z)$. Further, introducing the meromorphic matrices

$$M^+(x,t,z) = (\mu_{+,1}/s_{1,1},\, \mu_{-,2})\,, \qquad M^-(x,t,z) = (\mu_{-,1},\, \mu_{+,2}/s_{2,2})\,,$$

one obtains the jump condition

$$M^-(x,t,z) = M^+(x,t,z)\,(I - G(x,t,z))\,, \qquad z \in \Sigma\,, \tag{2.10}$$

where the jump matrix is

$$G(x,t,z) = \begin{pmatrix} 0 & -\mathrm{e}^{2i\theta(x,t,z)}\tilde{\rho}(z) \\ \mathrm{e}^{-2i\theta(x,t,z)}\rho(z) & \rho(z)\tilde{\rho}(z)\end{pmatrix}. \tag{2.11}$$

The asymptotic behavior of $M^\pm$ is as follows: $M^\pm = I + O(1/z)$ as $z \to \infty$ and $M^\pm = (i/z)\sigma_3 Q_- + O(1)$ as $z \to 0$, whereas $G(x,t,z)$ is $O(1/z)$ as $z \to \pm\infty$ and $O(z)$ as $z \to 0$ along the real axis. The above Riemann–Hilbert problem can be solved by subtracting the asymptotic behavior and the pole contributions (including the one at $z = 0$). Applying the modified Cauchy projectors yields a matrix singular linear integral equation for the solution of the Riemann–Hilbert problem:

$$M(x,t,z) = I + R(x,t,z) + \frac{1}{2\pi i}\int_\Sigma \frac{M^+(x,t,\xi)}{\xi - z}\,G(x,t,\xi)\,\mathrm{d}\xi\,, \tag{2.12}$$

where

$$R(x,t,z) = \frac{i}{z}\sigma_3 Q_- + \sum_{n=1}^{N}\left(\frac{\operatorname{Res}_{z_n} M^+}{z-z_n} + \frac{\operatorname{Res}_{-q_o^2/z_n^*} M^+}{z+q_o^2/z_n^*}\right) + \sum_{n=1}^{N}\left(\frac{\operatorname{Res}_{z_n^*} M^-}{z-z_n^*} + \frac{\operatorname{Res}_{-q_o^2/z_n} M^-}{z+q_o^2/z_n}\right).$$

To close the system, we need expressions for the residues. Let $\xi_n = z_n$ and $\xi_{n+N} = -q_o^2/z_n^*$ for $n = 1,\dots,N$. The residue relations give us

$$\operatorname{Res}_{\xi_n} M^+ = \left(C_n\,\mathrm{e}^{-2i\theta(x,t,\xi_n)}\mu_{-,2}(x,t,\xi_n)\,,0\right), \qquad n = 1,\dots,2N\,,$$
$$\operatorname{Res}_{\xi_n^*} M^- = \left(0\,,\tilde{C}_n\,\mathrm{e}^{2i\theta(x,t,\xi_n^*)}\mu_{-,1}(x,t,\xi_n^*)\right), \qquad n = 1,\dots,2N\,.$$

Evaluating the second column of (2.12) at $z = z_n$ and at $z = -q_o^2/z_n^*$ and the first column of (2.12) at $z = z_n^*$ and at $z = -q_o^2/z_n$ yields, for $n = 1,\dots,2N$,

$$\mu_{-,2}(x,t,\xi_n) = \begin{pmatrix} -iq_-/\xi_n \\ 1 \end{pmatrix} + \sum_{k=1}^{2N}\frac{\tilde{C}_k\,\mathrm{e}^{2i\theta(x,t,\xi_k^*)}}{\xi_n-\xi_k^*}\,\mu_{-,1}(x,t,\xi_k^*) + \frac{1}{2\pi i}\int_\Sigma \frac{M^+(x,t,\xi)}{\xi-\xi_n}\,G(x,t,\xi)\,\mathrm{d}\xi\,,$$

$$\mu_{-,1}(x,t,\xi_n^*) = \begin{pmatrix} 1 \\ iq_-^*/\xi_n^* \end{pmatrix} + \sum_{j=1}^{2N}\frac{C_j\,\mathrm{e}^{-2i\theta(x,t,\xi_j)}}{\xi_n^*-\xi_j}\,\mu_{-,2}(x,t,\xi_j) + \frac{1}{2\pi i}\int_\Sigma \frac{M^+(x,t,\xi)}{\xi-\xi_n^*}\,G(x,t,\xi)\,\mathrm{d}\xi\,.$$

The last task is to write the reconstruction formula, which is done using the asymptotic behavior of $M^\pm(x,t,z)$ as $z \to \infty$:

$$M(x,t,z) = I + \frac{1}{z}\left\{ i\sigma_3 Q_- + \sum_{n=1}^{2N}\left(\operatorname{Res}_{\xi_n} M^+ + \operatorname{Res}_{\xi_n^*} M^-\right) - \frac{1}{2\pi i}\int_\Sigma M^+(x,t,\xi)\,G(x,t,\xi)\,\mathrm{d}\xi \right\} + O(1/z^2)\,.$$

Comparing with (2.9), the reconstruction formula for the potential is obtained:

$$q(x,t) = q_- + i\sum_{n=1}^{2N}\tilde{C}_n\,\mathrm{e}^{2i\theta(x,t,\xi_n^*)}\,\mu_{-,1,1}(x,t,\xi_n^*) + \frac{1}{2\pi}\int_\Sigma (M^+G)_{1,2}(x,t,\xi)\,\mathrm{d}\xi\,. \tag{2.13}$$

3. One-soliton solutions. In the case of a reflectionless potential with one quartet of simple eigenvalues, the inverse problem yields a four-parameter family of solutions, depending on the location of the discrete eigenvalue. From the scaling symmetry of the NLS equation, we may set $q_o = 1$.

Consider first the case of a purely imaginary eigenvalue. Let $z_1 = iZ$, with $Z > 1$, and $C_1 = \mathrm{e}^{c_0+is_0}$, with $c_0, s_0 \in \mathbb{R}$. Then

$$q(x,t) = \frac{\cosh\chi + \frac{1}{2}c_+(1+c_-^2/c_+^2)\sin s - ic_-\cos s}{\cosh\chi + A\sin s}\,,$$

with $\chi(x,t) = c_- x + \chi_0$ and $s(x,t) = c_+ c_- t + s_0$, and where

$$c_\pm = Z \pm 1/Z\,, \qquad \chi_0 = \operatorname{arctanh}\left(\frac{c_+^2 - 4Z^2 c_-^2}{c_+^2 + 4Z^2 c_-^2}\right) + c_0\,, \qquad A = 2/c_+ < 1\,.$$

This solution was found by Kuznetsov in 1977 [36] and rediscovered by Ma [38] and others.

Translating the coordinates so the origin of the soliton is located at the origin and taking the limit $Z \to 1$ (i.e., the eigenvalue approaches the branch cut) yields the rational solution

$$q(x,t) = \frac{4x^2 - 16it + 16t^2 - 3}{4x^2 + 16t^2 + 1}\,,$$

which is referred to as the Peregrine soliton [42]. Note that this solution corresponds to a zero of $s_{1,1}(z)$ at $z = i$, i.e., along the continuous spectrum.

If we do not set $q_o = 1$ and take the limit $q_o \to 0$, we recover the one-soliton solution of the focusing NLS equation with ZBC. Explicitly, fixing the discrete eigenvalue at $z_1 = iZ$ and taking $q_o \to 0$ yields $q(x,t) = -i\,\mathrm{e}^{i(Z^2 t + \phi)} \operatorname{sech}[Zx + \log(2Z) + c_0] + O(q_o)$.

A discrete eigenvalue in general position yields the most general one-soliton solution. If we set $q_o = 1$ and write $z_1 = iZ\,\mathrm{e}^{i\alpha}$, with $Z > 1$ and $\alpha \in (-\pi/2, \pi/2)$, then

$$\begin{aligned} q(x,t) = \Big\{ &\cosh(\chi + 2i\alpha) + \frac{1}{2} A \left[c_{+2}\left(Z^2 \sin(s + 2\alpha) - \sin s\right)\right. \\ &\left. - i c_{-2}\left(Z^2 \cos(s + 2\alpha) - \cos s\right)\right] \Big\} \Big/ \Big\{ \cosh\chi + A\left[Z^2 \sin(s + 2\alpha) - \sin s\right] \Big\}\,, \end{aligned}$$

with $\chi(x,t) = c_- x \cos\alpha - c_{+2} t \sin(2\alpha) + \chi_0'$ and $s(x,t) = c_+ x \sin\alpha + c_{-2} t \cos(2\alpha) + s_0$, and where

$$\begin{aligned} c_{+2} &= Z^2 + 1/Z^2\,, \qquad c_{-2} = Z^2 - 1/Z^2 = c_+ c_-\,, \qquad A = 1/(c_+' c_-')\,, \\ c_+' &= |1 - Z^2\,\mathrm{e}^{-2i\alpha}|\,, \qquad c_-' = (Z + 1/Z)/(2\cos\alpha)\,, \qquad \chi_0' = \log(c_+'/c_-') + c_0\,, \end{aligned}$$

with $c_\pm$ as before. This solution was first derived by Tajiri and Watanabe in 1998 [44] and rediscovered recently by Zakharov and Gelash using the dressing method [49]. An example of such a solution is shown in Figure 2 (left).

Performing a translation of coordinates so that the maximum of the solution is at the origin and taking the limit $Z \to 1$ yields the so-called Akhmediev breathers [33]

$$q(x,t) = \frac{\cosh[2\sin(2\alpha)t - 2i\alpha] - \cos\alpha\,\cos[2\sin(\alpha)x]}{\cosh[2\sin(2\alpha)t] - \cos\alpha\,\cos[2\sin(\alpha)x]}\,.$$

Note, however, that a zero of the analytic scattering coefficient on the branch cut is not a true discrete eigenvalue because the zero is on the continuous spectrum. Thus the eigenfunctions oscillate as $x \to \pm\infty$, instead of decaying as in the case of a proper eigenvalue. The corresponding solutions, which are obtained by taking the limit of the eigenvalue to the branch cut, are periodic in x and are therefore outside the scope of the IST presented in section 2. An example of such a solution is shown in Figure 2 (right).

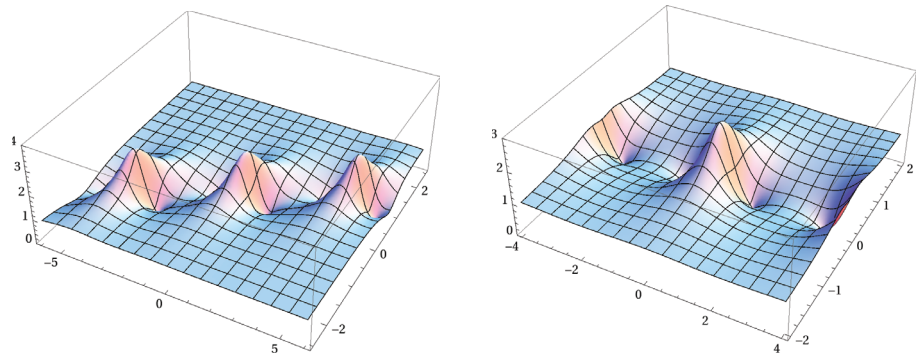

FIG. 2. *Left: The modulus $|q(x,t)|$ of a traveling one-soliton solution of the focusing NLS equation with NZBC as a function of x and t with $q_o = 1$ and a discrete eigenvalue $z_1 = \sqrt{2}\,\mathrm{e}^{i\pi/4}$, resulting in an asymptotic phase difference $\theta_+ - \theta_- = \pi$. Right: The same for an Akhmediev breather, obtained for $\alpha = \pi/4$.*

4. Piecewise-constant potentials. We now consider IVPs for the focusing NLS equation (2.1) with the following piecewise-constant, box-like IC with nonzero background:

$$q(x,0) = \begin{cases} 1\,, & |x| > L\,, \\ b\,\mathrm{e}^{i\alpha}\,, & |x| < L\,. \end{cases} \tag{4.1}$$

This will allow us to infer various general results about the case with NZBC in section 5 (similarly in spirit to the work of Satsuma and Yajima [43] for the NLS equation with ZBC). Due to the scaling and phase symmetries of the NLS equation, we may set $q_- = 1$ in (4.1). The parameter $b > 0$ quantifies the height of the potential inside the box. The case $0 < b < 1$ represents a potential well and the case $b > 1$ a potential barrier. The parameter α represents the phase difference between the value of the potential inside the box and its background value.

Since the scattering matrix is time-independent, it suffices to evaluate the Jost eigenfunctions at $t = 0$. Owing to the piecewise constant nature of the initial condition (4.1), the Jost solutions at $t = 0$ have a simple representation in certain subsets of the real axis. Namely,

$$\phi_-(x,0,k) = \left(I + \frac{i}{k+\lambda}\sigma_3 Q_-\right)\mathrm{e}^{i\lambda x\sigma_3}, \qquad x < -L\,, \tag{4.2a}$$

$$\phi_+(x,0,k) = \left(I + \frac{i}{k+\lambda}\sigma_3 Q_+\right)\mathrm{e}^{i\lambda x\sigma_3}, \qquad x > L\,. \tag{4.2b}$$

In addition, a fundamental matrix solution of the scattering problem in the central region is

$$\phi_0(x,0,k) = \left(I + \frac{i}{k+\mu}\sigma_3 Q_0\right)\mathrm{e}^{i\mu x\sigma_3}, \qquad |x| < L\,, \tag{4.2c}$$

where

$$\mu^2 = k^2 + b^2\,. \tag{4.3}$$

Note that, in this section and the next, it will be convenient to express the Jost eigenfunctions and the scattering coefficients in terms of the original scattering parameter k instead of the uniformization variable z. We will choose the value of $\lambda(k)$ corresponding to the first sheet of the Riemann surface. In particular, $\operatorname{Re}\lambda(k)$ and $\operatorname{Im}\lambda(k)$ will both be positive in the first quadrant of the complex k-plane.

The expressions of the above eigenfunctions beyond the domains in (4.2) are obtained by requiring continuity at the boundary. Each of the eigenfunctions in (4.2) is a fundamental matrix solution of the scattering problem for $k \in \mathbb{C} \setminus \{\pm i, \pm ib\}$. (Since the IC (4.1) have effectively compact support, the eigenfunctions have larger regions of analyticity than for generic potentials.) Thus, there are matrices $S_\pm(k)$, independent of x and t, such that

$$S_+(k) = \phi_o^{-1}(x,t,k)\phi_+(x,t,k)\,, \quad S_-(k) = \phi_o^{-1}(x,t,k)\phi_-(x,t,k)\,. \tag{4.4}$$

The scattering matrix is then given by $S(k) = S_-^{-1}(k)S_+(k)$. We may determine $S_\pm(k)$ by evaluating (4.4) at $x = \pm L$, respectively, and $t = 0$. In particular,

$$s_{1,1}(k) = \mathrm{e}^{2iL\lambda}\left(\cos(2L\mu) - \frac{i(b\cos\alpha + k^2)}{\lambda\mu}\sin(2L\mu)\right). \tag{4.5}$$

Note that $s_{1,1}(k)$ is an even function of $\mu(k)$, so it is independent of the choice of sign in (4.3).

In section 5 we will use (4.5) to characterize the discrete spectrum of the potential well and potential barrier by finding the zeros of $s_{1,1}(k)$ in the upper half-plane—including the branch cut. Note that $s_{1,1}$ is singular when $\lambda = 0$ or $\mu = 0$ (i.e., for $k = i$ and $k = ib$, respectively). Evaluating (4.5) at $k = i$ and at $k = ib$, we see that $s_{1,1}$ has a pole at $k = i$ and a removable singularity at $k = ib$. Thus, we seek those values of $k \in \mathbb{C}^+ \setminus \{i, ib\}$ such that

$$\lambda\mu\cos(2\mu L) = i(b\cos\alpha + k^2)\sin(2\mu L) \tag{4.6}$$

or, equivalently,

$$\mathrm{e}^{2iL\mu}(\lambda\mu - b\cos\alpha - k^2) + \mathrm{e}^{-2iL\mu}(\lambda\mu + b\cos\alpha + k^2) = 0\,. \tag{4.7}$$

It will be useful to define

$$F(k) = \mathrm{e}^{2iL\mu}\tilde{F}(k)\,, \qquad \tilde{F}(k) = \lambda\mu - b\cos\alpha - k^2\,, \tag{4.8a}$$

$$G(k) = \mathrm{e}^{-2iL\mu}\tilde{G}(k)\,, \qquad \tilde{G}(k) = \lambda\mu + b\cos\alpha + k^2\,. \tag{4.8b}$$

Also note that, since the potential (4.1) is even, the IVP is equivalent to an initial-boundary value problem on the half-line with homogeneous Neumann boundary conditions. For decaying potentials at infinity, such problems were studied in [5, 10, 11, 9, 22, 32, 45]. In Appendix B we discuss the extension of those results to the case of potentials with NZBC at infinity. In particular, we show that $s_{1,1}(k)$ obeys the symmetry

$$s_{1,1}(k) = s_{1,1}^*(-k^*)\,, \qquad k \in \overline{\mathbb{C}_\mathrm{I}} \setminus i[0,1]\,, \tag{4.9}$$

where from now on $\mathbb{C}_\mathrm{I}$ denotes the interior of the first quadrant of the complex k-plane and $\overline{\mathbb{C}_\mathrm{I}}$ its closure. As a result, we may restrict our search to $k \in \overline{\mathbb{C}_\mathrm{I}}$. Of course,

$\lambda(k)$ has a sign discontinuity across the branch cut $k \in i[0,1]$, and therefore $s_{1,1}(k)$ is discontinuous there as well. Since we defined $\lambda(k)$ to be continuous from the right, $s_{1,1}(k)$ is, too. (So for $k \in i[0,1]$, (4.9) should be intended as a limit.) Finally, it will be useful to define the quantity

$$b_\alpha = \begin{cases} \sqrt{b\cos\alpha}\,, & \cos\alpha \geq 0\,, \\ -i\sqrt{-b\cos\alpha}\,, & \cos\alpha < 0\,. \end{cases} \tag{4.10}$$

Note that b_α is real when $\cos\alpha > 0$, but it is imaginary when $\cos\alpha < 0$.

5. Discrete spectrum. We now use the expressions derived in section 4 to characterize the spectrum of the scattering problem for the focusing NLS equation with NZBC. We will study the case of the potential well and potential barrier separately. Proofs for the theorems in this section can be found in Appendix C. A summary of the results is provided in section 5.5.

5.1. Potential well, small phase difference. Recall that for the potential well $b < 1$. We first consider the case $\cos\alpha > b$, implying $b_\alpha > b$. The case of $\cos\alpha < b$ will be considered in section 5.3. We use Rouché's theorem on the first quadrant of the complex k-plane to prove the following.

THEOREM 5.1. *If $0 < b < 1$ and $\cos\alpha > b$ (i.e., $b_\alpha > b$), the scattering problem has no discrete eigenvalues.*

Remark. We emphasize that Theorem 5.1 is particularly significant to the efforts to understand the nonlinear stage of the MI. It was recently conjectured that the mechanism underlying the MI is the creation of soliton-antisoliton pairs [49]. However, since there exists a class of perturbations of the constant background that admit no discrete spectrum, soliton creation *cannot* be the main mechanism responsible for the MI, because *all* perturbations of the constant background are linearly unstable. However, the IST does provide a key insight into the issue. The vehicle for the MI within the context of the IST will be discussed in section 6.

5.2. Potential barrier, small phase difference. We now consider the case of a barrier-type potential, in which $b > 1$. In this section, we restrict ourselves to the case $\cos\alpha > 1/b$, implying $b_\alpha > 1$. We first study the existence of discrete eigenvalues on the imaginary axis.

THEOREM 5.2. *If $b > 1$ and $\cos\alpha > 1/b$ (i.e., $b_\alpha > 1$), the scattering problem has at least one discrete eigenvalue in the segment $i(1,b)$ of the imaginary axis.*

Remark. The proof of Theorem 5.2 shows that the scattering problem acquires an additional eigenvalue at $L = n\pi/(2\sqrt{b^2-1})$ for each integer value of n. Thus, these are the bifurcation points. Moreover, analysis also shows that all these eigenvalues bifurcate from the point $\mu = \sqrt{b^2-1}$, i.e., from $k = ib$. Also, a direct consequence of Theorem 5.2 is the following.

COROLLARY 5.3. *No area theorem is possible for the focusing NLS equation with NZBC.*

Remark. Recall that an area theorem is a condition on the initial condition for the existence of discrete eigenvalues. In the case of the focusing NLS equation with ZBC, one can show that if $\int_{-\infty}^{\infty} |q(x,0)|\,\mathrm{d}x < \pi/2$, the scattering problem has no discrete eigenvalues [2, 35]. On the other hand, for the Korteweg–deVries equation no such area theorem is possible, since discrete eigenvalues can exist for arbitrarily small potentials [28]. For the focusing NLS equation with NZBC, we may think of the requirement $\cos\alpha > 1/b$ as a condition on the distance between the background

and the box. Pointwise, for all $-L < x < L$,

$$d(q(x,0),1) = \sqrt{b^2 - 2b\cos\alpha + 1} < \sqrt{b^2 - 1}\,.$$

On the other hand, setting $\alpha = 0$, Theorem 5.2 implies that discrete eigenvalues exist for L arbitrarily close to 0 and b arbitrarily close to 1, implying that no area theorem is possible for the focusing NLS equation with NZBC. This situation is similar to that of the defocusing NLS equation with NZBC [13].

By using an approach similar to the proof of Theorem 5.1, we will also show that the eigenvalues in $i(1,b)$ are the only discrete eigenvalues.

THEOREM 5.4. *If $b > 1$ and $\cos\alpha > 1/b$ (i.e., $b_\alpha > 1$), the scattering problem has no discrete eigenvalues off the interval $i(1,b)$.*

5.3. Potential well, large phase difference. We return to the potential well to consider the case of a large phase difference between the background and the potential inside the box. We begin by considering $i(1,\infty)$.

THEOREM 5.5. *If $0 < b < 1$ and $\cos\alpha \le b$, the scattering problem has no purely imaginary discrete eigenvalues.*

Remark. Theorem 5.5 leaves open the possibility that $s_{1,1}(k)$ admits zeros along the continuous spectrum or in the interior of the first quadrant. Regarding the former possibility, we may use the argument from the proof of Theorem 5.1 (along segment 4) to show that $s_{1,1}(k) \neq 0$ for $k \in i(b,1)$. Thus, any zeros of $s_{1,1}(k)$ on the continuous spectrum lie either along $k \in \mathbb{R}^+$ or on the imaginary axis between $k = 0$ and $k = ib$.

LEMMA 5.6. *If $0 < b < 1$, $\cos\alpha < b$, and $L = [(2n+1)\pi]/[4\sqrt{b^2 - b_\alpha^2}]$, the scattering problem has a single zero on the continuous spectrum at $k = ib_\alpha$.*

Remarks. (i) The proof of Lemma 5.6 shows there are no zeros of $s_{1,1}(k)$ along the continuous spectrum for all other values of L. (ii) When $\cos\alpha < 0$, b_α is purely imaginary, and the zero is along the positive real axis. When $\cos\alpha > 0$, b_α is real, and the zero is on the imaginary axis, corresponding to a so-called Akhmediev breather. In either of these two cases, such a zero is not a discrete eigenvalue of the scattering problem, since the corresponding eigenfunctions are not in $L^2(\mathbb{R})$.

Remark. Regarding the existence of discrete eigenvalues in the interior of the first quadrant, unfortunately we were unable to obtain any rigorous conclusions. On the other hand, numerical evidence shows that such eigenvalues can exist (see Figure 3). Specifically, we observe that $|G| - |F|$ is a continuous function on $\overline{\mathbb{C}}_{\mathrm{I}}$. In the case of $0 < \cos\alpha < b$, this function is negative on $i(b_\alpha, b)$ and positive on $(i\mathbb{R} \setminus i[b_\alpha, b]) \cup \mathbb{R}$. In the case of $\cos\alpha < 0$, this function is positive on $(i\mathbb{R} \setminus i[0,b]) \cup (\mathbb{R} \setminus [0, \sqrt{-b\cos\alpha}])$ and negative on $i[0,b) \cup [0, \sqrt{-b\cos\alpha})$. Thus, there is a contour in $\mathbb{C}_{\mathrm{I}}$ with endpoints ib and ib_α on which $|F| = |G|$. The eigenvalues bifurcate from $k = ib_\alpha$ when $L = (2n+1)\pi/(4\sqrt{b^2 - b_\alpha^2})$. Numerical evidence suggests that as L further increases, the discrete eigenvalue travels upwards along the contour given by $|G| = |F|$, getting arbitrarily close to $k = ib$. At the next odd multiple of $\pi/(4\sqrt{b^2 - b_\alpha^2})$, an additional eigenvalue appears at $k = ib_\alpha$. The eigenvalues accumulate at $k = ib$.

5.4. Potential barrier, large phase difference. Finally, we return to the case of a potential barrier, i.e., $b > 1$, but now with $\cos\alpha < 1/b$. As in the case of the well, there are generically no zeros on the continuous spectrum. However, for $L = (2n+1)\pi/(4\sqrt{b^2 - b_\alpha^2})$, the scattering problem has a single zero on the continuous spectrum at $k = ib_\alpha$, where $ib_\alpha \in \mathbb{R}$ if $\cos\alpha < 0$. (The proof of this statement is the

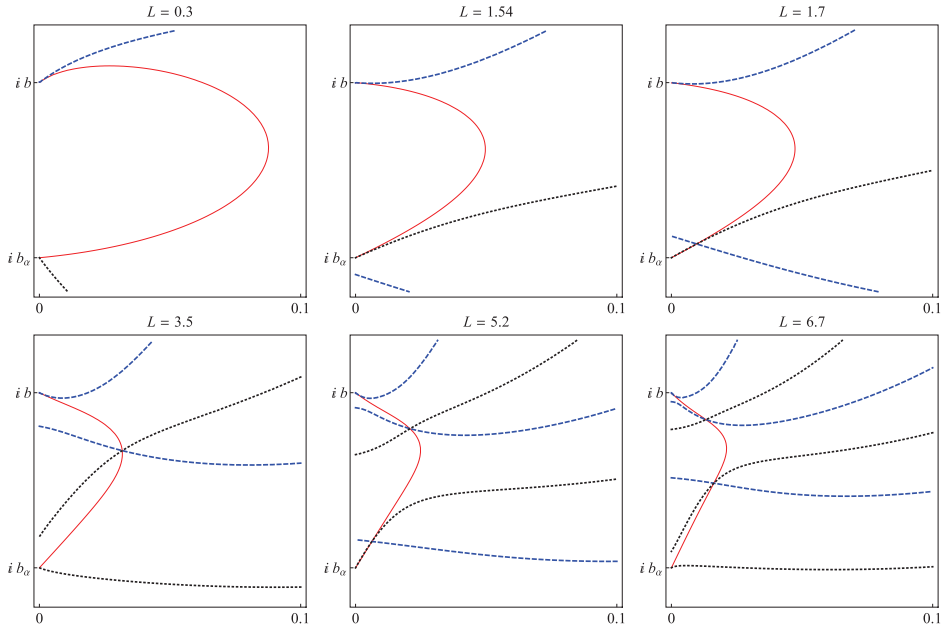

FIG. 3. *Location of discrete eigenvalues in the complex k-plane for a potential well with $b = 0.8$, $\alpha = \pi/3$, and various values of L. Solid contours (in red online): locus of $|F(k)| = |G(k)|$. Dashed contours (in blue online): level curves* $\mathrm{Re}[F(k) + G(k)] = 0$. *Dotted black contours: level curves* $\mathrm{Im}[F(k) + G(k)] = 0$. *The intersection of the latter two yields the discrete eigenvalues. At each odd multiple of $l = \pi/(4\sqrt{b^2 - b_\alpha^2}) = 1.603$ a discrete eigenvalue appears at $k = ib_\alpha = 0.632\,i$. As L increases, the discrete eigenvalue travels upwards along the red contour, accumulating near $k = ib$. At the next odd multiple of l, an additional eigenvalue appears at $k = ib_\alpha$.*

same as that of Lemma 5.6.) Next we look for zeros $k = iy$, $1 < y < b$.

LEMMA 5.7. *Let*

$$\ell_n(y) = \frac{1}{2\sqrt{b^2 - y^2}} \left[n\pi + \operatorname{arccot}\left(\frac{b\cos\alpha - y^2}{\sqrt{b^2 - y^2}\sqrt{y^2 - 1}} \right) \right],$$

where the branch of arccotangent is chosen to have range $(0, \pi)$. For all $1 < y < b$ and $n \in \mathbb{N}_0$, if $L = \ell_n(y)$, the scattering problem has a discrete eigenvalue at $k = iy$.

By examining the range of $\ell_n(y)$, we find further conditions on L which guarantee the existence of an imaginary discrete eigenvalue.

THEOREM 5.8. *The scattering problem for the potential barrier contains a purely imaginary discrete eigenvalue if any of the following hold:*

(i) $\cos\alpha > 1/b$,
(ii) $\cos\alpha = 1/b$ *and* $L > \pi/(4\sqrt{b^2 - 1})$,
(iii) $\cos\alpha < 1/b$ *and* $L > \pi/(2\sqrt{b^2 - 1})$.

The three situations are illustrated in Figure 4.

Remark. Note that the conditions in Theorem 5.8 are sufficient but not necessary for the existence of eigenvalues in $i(1, b)$, as can be seen in Figure 4(a), for which discrete eigenvalues exist even for values of L smaller than the bound in Theorem 5.8 (depicted by a gray dot-dashed line). To find the bifurcation point (i.e., the value of L at which eigenvalues appear), one needs to minimize $L = \ell_0(y)$ as a function of y in the interval $(1, b)$. The function $\ell_0(y)$ is continuously differentiable, so either the minimum occurs when $d\ell/dy = 0$, or there is no local minimum and we consider

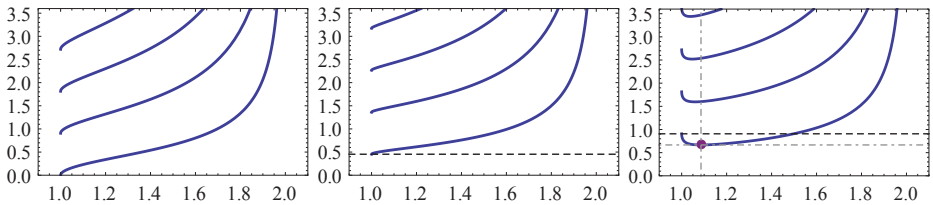

FIG. 4. *Bifurcation plots for the discrete spectrum $k = iy$ of the potential barrier with $b = 2$ and $\alpha = 0$ (left), $\alpha = \pi/3$ (center), and $\alpha = 2\pi/5$ (right), as a function of y (horizontal axis) and L (vertical axis). The dashed line is at $L = \pi/(2\sqrt{3})$ (right) and $L = \pi/(4\sqrt{3})$ (center). When $b_\alpha > 1$ (left), there is a discrete eigenvalue for all values of L, as discussed in section 5.2. When $b_\alpha = 1$ (center), there is a discrete eigenvalue if and only if $L > \pi/(4\sqrt{b^2-1})$. Finally, when $b_\alpha < 1$, i.e., when $\cos\alpha < 1/b$ (right), $L > \pi/(2\sqrt{b^2-1})$ ensures the existence of at least one discrete eigenvalue, but the latter is not a necessary condition.*

$y \to 1^+$. Differentiating $\ell_0(y)$ and setting $d\ell_0/dy = 0$, we see that the bifurcation point is given by the solution of the transcendental equation

$$\frac{-p(y)}{\sqrt{r(y)}} = \cot\left(\frac{2r(y) + p(y)(b^2+1-2y^2)}{r(y)+p(y)^2}\sqrt{\frac{b^2-y^2}{y^2-1}}\right), \tag{5.1}$$

where $p(y) = b\cos\alpha - y^2$ and $r(y) = (b^2-y^2)(y^2-1)$. One can solve this equation numerically for y. For example, for $b = 1.25$ and $\alpha = \pi/3$, a solution is $y_o = 1.021$, corresponding to $L = 1.941$. Such a case is illustrated in the top center plot of Figure 5.

Remark. As in the case of a potential well with a large phase difference, we were unable to obtain rigorous results concerning the number and location of discrete eigenvalues in the interior of the first quadrant. On the other hand, numerical evidence suggests that a discrete eigenvalue appears at $k = ib_\alpha$ when $L = (2n+1)\pi/(4\sqrt{b^2-b_\alpha^2})$. As L increases, the eigenvalue travels along the contour given by $|G| = |F|$. Then at $L(y_o)$—where y_o solves the transcendental equation (5.1)—the eigenvalue bifurcates into two eigenvalues. Both move along the imaginary axis: one travels down and disappears at $k = i$, and the other becomes arbitrarily close to $k = ib$, as can be seen in the top center and right plots of Figure 5 (as well as in the right-hand plot of Figure 4).

5.5. Summary. We summarize the findings for the various IC studied in this section.

1. For a potential well with $\cos\alpha > b$ there are no discrete eigenvalues $s_{1,1}(k)$ (nor zeros of $s_{1,1}(k)$ along the continuous spectrum). In particular, this shows that solitons cannot be the primary vehicle for the nonlinear stage for MI.
2. For a potential well with $\cos\alpha < b$, there is a zero of $s_{1,1}(k)$ on the continuous spectrum at ib_α whenever $L = (2n+1)L_\alpha$, where $L_\alpha = \pi/(4\sqrt{b^2-b_\alpha^2})$. There are no other zeros on the real or imaginary axes. Numerical evidence suggests that as L increases, the discrete eigenvalues travel away from ib_α along a contour in the first quadrant, accumulating at ib.
3. For a potential barrier with $\cos\alpha > 1/b$, there is always at least one discrete eigenvalue in $i(1,b)$. In particular, this shows that no area theorem is possible for the focusing NLS equation with NZBC. More precisely, for $(n-1)L_o < L < nL_o$, where $L_o = \pi/(2\sqrt{b^2-1})$, there are exactly n discrete eigenvalues

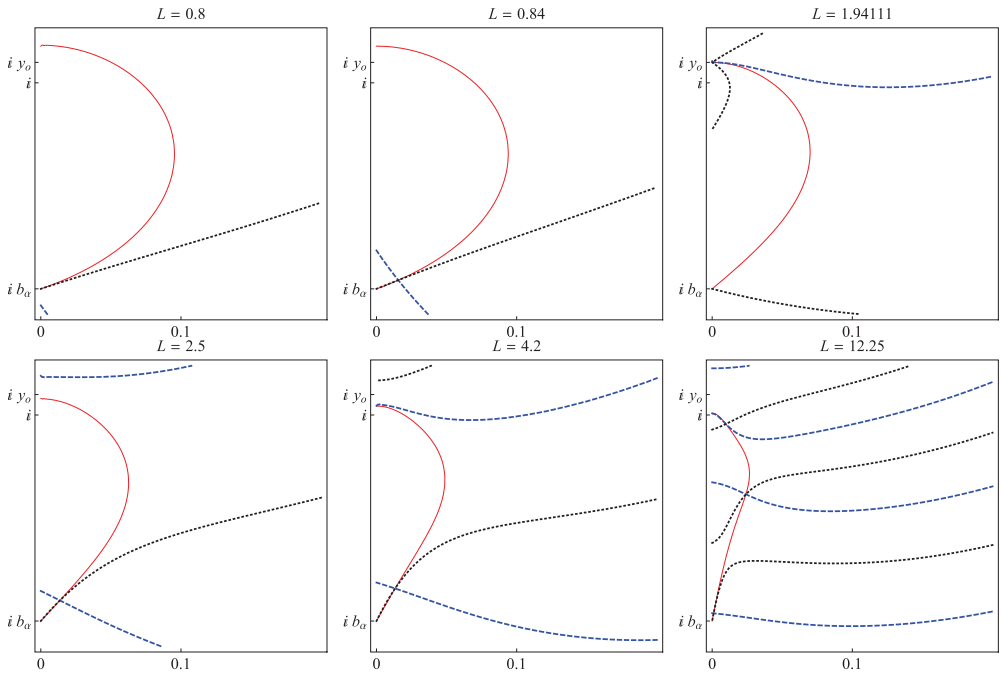

FIG. 5. *Location of discrete eigenvalues in the complex k-plane for a potential barrier with $b = 1.25$, $\alpha = \pi/3$, and various values of L. Solid contours (in red online): locus of $|F(k)| = |G(k)|$. Dashed contours (in blue online): level curves* $\mathrm{Re}[F(k) + G(k)] = 0$. *Dotted black contours: level curves* $\mathrm{Im}[F(k)+G(k)] = 0$. *At each odd multiple of $l = \pi/(4\sqrt{b^2 - b_\alpha^2}) = 0.811$ a discrete eigenvalue appears at $k = ib_\alpha = 0.791\,i$. As L further increases, the discrete eigenvalue travels upwards along the red contour. When it reaches iy_o, where $y_o = 1.021$ solves* (5.1) *and $L(y_o) = 1.941$, it bifurcates into two eigenvalues which travel along the imaginary axis. One eigenvalue travels down from iy_o, disappearing at i, and one eigenvalue travels upwards, getting arbitrarily close to ib. This can be seen in the left-hand plot of Figure* 4, *where y_o represents the minimum of the first (lowest) curve.*

in $i(1, b)$, and these eigenvalues accumulate near ib (on the imaginary axis) as L increases. Moreover, there are no other discrete eigenvalues.

4. For a potential barrier with $\cos\alpha \leq 1/b$, if $L > \pi/(2\sqrt{b^2 - 1})$ there is at least one discrete eigenvalue in $i(1, b)$. If $\cos\alpha < 1/b$, then, as with the potential well, $s_{1,1}(k)$ has a zero on the continuous spectrum at ib_α whenever $L = (2n+1)L_\alpha$. Numerical evidence suggests that as L increases, the discrete eigenvalues travel in the first quadrant of the complex plane, bifurcating at points in $i(1, b)$. After bifurcating, eigenvalues traveling downwards disappear at the branch point (i.e., $k = i$); those traveling upwards accumulate at $k = ib$.

6. Comparison between the IST and the linearization of the NLS equation. We now take the limit of the IST when the IC are a small deviation of the constant background, and we show that, modulo the possible contribution of the discrete eigenvalues, the solution in this limit coincides exactly with that of the direct linearization of the NLS equation around the constant background. We begin by briefly reviewing the latter.

6.1. Direct linearization of the NLS equation for small-deviation IC. Given any solution $q_s(x, t)$ of the NLS equation (2.1), one can study the evolution of a small perturbation to it by seeking a solution in the form $q(x, t) = q_s(x, t) + v(x, t)$.

The solution is linearly stable if $v(x,0) = O(\varepsilon)$ implies $v(x,t) = O(\varepsilon)$ for all $t > 0$. In particular, taking $q(x,t) = q_o + v(x,t)$ (with $q_o > 0$), substituting in the NLS equation, and keeping $O(\varepsilon)$ terms, one obtains the linearization of the NLS equation around the constant background:

$$iv_t + v_{xx} - 2\nu q_o^2(v + v^*) = 0\,.$$

It is convenient to define $r = v + v^*$ and $is = v - v^*$, which satisfy

$$r_t + s_{xx} = 0\,, \qquad s_t - r_{xx} + 4\nu q_o^2 r = 0.$$

This system may be solved with Fourier transforms. Introducing $\hat{r}(\zeta,t) = \mathcal{F}_\zeta[r(x,t)]$ and $\hat{s}(\zeta,t) = \mathcal{F}_\zeta[s(x,t)]$ (defined in (A.2)), as well as $\hat{\mathbf{r}}(\zeta,t) = (\hat{r},\hat{s})^T$, yields

$$\hat{\mathbf{r}}_t = \begin{pmatrix} 0 & \zeta^2 \\ -\zeta^2 - 4\nu q_o^2 & 0 \end{pmatrix} \hat{\mathbf{r}}\,. \tag{6.1}$$

The eigenvalues of this system are $\pm i\gamma(\zeta)$, where $\gamma(\zeta) = \zeta\sqrt{\zeta^2 + 4\nu q_o^2}$. The stability of the background depends on the sign of ν. If $\nu = 1$ (defocusing case), $\gamma(\zeta)$ is real for all real ζ, so an initially small perturbation remains small. In this case plane waves are stable. If $\nu = -1$ (focusing case), $\gamma(\zeta)$ becomes imaginary for $\zeta \in (-2q_o, 2q_o)$, so an initially small perturbation will grow exponentially. Thus, in the focusing case, plane waves are unstable to long wavelength perturbations. One can estimate the growth rate of the perturbations from the maximum of $|\operatorname{Im}\gamma(\zeta)|$, which occurs at $\zeta = \sqrt{2}q_o$, where $|\operatorname{Im}\gamma(\zeta)| = 2q_o$.

The solution of (6.1) with $\nu = -1$ is

$$\hat{\mathbf{r}}(\zeta,t) = \left[\cos(\gamma(\zeta)t) + \begin{pmatrix} 0 & \zeta^2/\gamma(\zeta) \\ -\gamma(\zeta)/\zeta^2 & 0 \end{pmatrix} \sin(\gamma(\zeta)t)\right] \hat{\mathbf{r}}(\zeta,0)\,. \tag{6.2}$$

The expression in brackets is real for all $\zeta \in \mathbb{R}$, but the trigonometric functions become hyperbolic for $\zeta \in (-2q_o, 2q_o)$. Reconstructing $v(x,t) = \frac{1}{2}(r(x,t) + is(x,t))$ yields the solution of the linearized NLS equation:

$$v(x,t) = \frac{1}{2\pi}\int_{\mathbb{R}} \mathrm{e}^{i\zeta x}\hat{v}(\zeta,t)\,\mathrm{d}\zeta\,, \tag{6.3a}$$

where

$$\hat{v}(\zeta,t) = \left[\cos(\gamma(\zeta)t) + \frac{i(2q_o^2 - \zeta^2)}{\gamma(\zeta)}\sin(\gamma(\zeta)t)\right]\hat{v}(\zeta,0) + \frac{2iq_o^2}{\gamma(\zeta)}\sin(\gamma(\zeta)t)\hat{v}^*(\zeta,0)\,. \tag{6.3b}$$

Performing the change of variables $\zeta = 2\lambda$ and writing $k = \sqrt{\lambda^2 - q_o^2}$, (6.3) becomes

$$\begin{aligned} v(x,t) = \frac{1}{2\pi}\int_{\mathbb{R}} \mathrm{e}^{2i\lambda x}\Bigg[&\mathrm{e}^{-4i\lambda kt}\left[\frac{(\lambda+k)^2}{2\lambda k}\hat{v}(2\lambda,0) - \frac{q_o^2}{2\lambda k}\hat{v}^*(2\lambda,0)\right] \\ &+ \mathrm{e}^{4i\lambda kt}\left[-\frac{(\lambda-k)^2}{2\lambda k}\hat{v}(2\lambda,0) + \frac{q_o^2}{2\lambda k}\hat{v}^*(2\lambda,0)\right]\Bigg]\mathrm{d}\lambda\,. \end{aligned} \tag{6.4}$$

We next show how, in the small-deviation limit, the results of the IST coincide with these expressions, apart from the possible contributions of the discrete spectrum.

6.2. Small-deviation limit of the IST. We now consider $q(x,t) \to q_o$ as $x \to \pm\infty$, that is, $q_\pm = q_o$. In this case $Y_+ = Y_- = I + (iq_o/z)\sigma_1 =: Y$ and $\Delta Q_+ = \Delta Q_- =: \Delta Q$. The integral equations for the modified eigenfunctions become

(6.5a)
$$\mu_+(x,t,z) = Y(z) - \int_x^\infty Y\,\mathrm{e}^{i\lambda(z)(x-y)\sigma_3}\,Y^{-1}\,\Delta Q(y,t)\,\mu_+(y,t,z)\,\mathrm{e}^{-i\lambda(z)(x-y)\sigma_3}\mathrm{d}y\,,$$

(6.5b)
$$\mu_-(x,t,z) = Y(z) + \int_{-\infty}^x Y\,\mathrm{e}^{i\lambda(z)(x-y)\sigma_3}\,Y^{-1}\,\Delta Q(y,t)\,\mu_-(y,t,z)\,\mathrm{e}^{-i\lambda(z)(x-y)\sigma_3}\mathrm{d}y\,.$$

Combining (6.5) with(2.7) yields

$$S(z) = I - \int_{\mathbb{R}} \mathrm{e}^{-i\theta(y,t,z)\sigma_3}\,Y^{-1}(z)\,\Delta Q(y,t)\,\mu_+(y,t,z)\mathrm{e}^{i\theta(y,t,z)\sigma_3}\mathrm{d}y\,. \tag{6.6}$$

We evaluate the limit of the IST when $q(x,t) - q_o = O(\varepsilon)$. Note that if $\Delta Q = O(\varepsilon)$, then $\mu_\pm(x,t,z) = Y + O(\varepsilon)$ and $S(z) = I + O(\varepsilon)$. (Moreover, we may evaluate the above expression at $t = 0$ since $S(z)$ is independent of t.) In particular,

$$s_{1,2}(z) = \frac{1}{q_o^2 + z^2}\int_{\mathbb{R}} \mathrm{e}^{-2i\lambda(z)y}\,\left(-z^2\Delta q(y,0) + q_o^2\Delta q^*(y,0)\right)\,\mathrm{d}y + O(\varepsilon^2)\,. \tag{6.7}$$

One can expect that, as $\varepsilon \to 0$, at most one discrete eigenvalue is present. Neglecting this possible contribution from the discrete spectrum, the reconstruction formula (2.13) is

$$q(x,t) = q_o - \frac{1}{2\pi}\int_\Sigma \mathrm{e}^{2i\theta(x,t,z)}\,s_{1,2}(z)\,\mathrm{d}z + O(\varepsilon^2)\,. \tag{6.8}$$

In order to compare this expression with that obtained from the linearization it is necessary to perform a few changes of variable using (2.5). Different portions of the integration contour (see Figure 1 (left)) will correspond to different changes of variable. We observe, for example, that $z \in (q_o, \infty)$ and $z \in (0, q_o)$ both correspond to $\lambda \in (q_o, \infty)$, but k changes sign. In the same way, both the upper and lower halves of C_o correspond to $\lambda \in [-q_o, q_o]$, but again, they represent different signs for k. Thus we must consider the change of variable $z = \lambda + \sqrt{\lambda^2 - q_o^2}$ or $z = \lambda - \sqrt{\lambda^2 - q_o^2}$ depending on the portion of the integration contour. After doing so, and with some abuse of notation, (6.8) becomes

$$\begin{aligned} q(x,t) = q_o &- \frac{1}{2\pi}\int_{\mathbb{R}} \mathrm{e}^{2i\lambda(x-2kt)}\,s_{1,2}(\lambda,k)\frac{\lambda+k}{k}\,\mathrm{d}\lambda \\ &+ \frac{1}{2\pi}\int_{\mathbb{R}} \mathrm{e}^{2i\lambda(x+2kt)}\,s_{1,2}(\lambda,-k)\frac{\lambda-k}{k}\,\mathrm{d}\lambda + O(\varepsilon^2)\,. \end{aligned} \tag{6.9}$$

From (6.7) we have

$$s_{1,2}(\lambda,k) = -\frac{k+\lambda}{2\lambda}\hat{v}(2\lambda,0) + \frac{1}{2\lambda(k+\lambda)}\hat{v}^*(2\lambda,0) + O(\varepsilon^2)\,. \tag{6.10}$$

Combining (6.9) with (6.10), we see that $q(x,t) = q_o + v(x,t) + O(\varepsilon^2)$ as $\varepsilon \to 0$, where $v(x,t)$ is precisely as in (6.4). In other words, modulo the contribution from

the discrete eigenvalues, the small-deviation limit of IST coincides exactly with the linearization of the NLS equation around a constant background.

At this point it is crucial to realize that, even though the branch cut lies in the imaginary axis, the corresponding Jost eigenfunctions of the scattering problem are still bounded with respect to x. This is because their asymptotic spatial oscillations are determined by $\lambda(k)$, which is also real-valued on the branch cut. (Recall that the boundary conditions for the Jost eigenfunctions are given in terms of $\theta(x,t,k) = \lambda(k)x - \omega(k)t$; see (2.6).) Thus, just like in the case of ZBC, *even these Jost eigenfunctions are the nonlinearization via IST of genuine Fourier modes.* On the other hand, the temporal dependence of the asymptotic boundary conditions for the Jost eigenfunctions is governed by $2\omega(k) = 4k\lambda(k)$. On the branch cut, $\omega(k)$ is purely imaginary. Indeed, modulo trivial rescalings, $\operatorname{Im}\omega(k)$ is precisely the growth rate of the unstable Fourier modes in the linearized NLS equation! Moreover, the above comparison between the small-deviation limit of IST and the linearization shows that, in this limit, the contribution from the Jost eigenfunctions along the branch cut coincides exactly with that of the unstable Fourier modes in the linearization.

7. Discussion. The results of this work show how the IST provides a natural mechanism for the saturation of the MI. To illustrate this point, it is useful to briefly look at how the results fit within the broader context of the IST.

It is well known that, for integrable nonlinear PDEs with suitably localized IC, the IST is the nonlinear analogue of the Fourier transform method. In the latter, the IC are decomposed into a linear superposition of frequency components, each with its own amplitude and phase, which then evolve independently as plane waves with their own phase velocity. In the IST, the role of these plane waves is played by the Jost eigenfunctions, which indeed reduce to plane waves in the appropriate asymptotic limit (i.e., $x \to -\infty$ or $x \to \infty$) for all values of the spectral parameter on the continuous spectrum. On the other hand, when a discrete spectrum is present, the solution of the nonlinear PDE contains contributions from the Jost eigenfunctions evaluated at values of the spectral parameter off the continuous spectrum. The asymptotic behavior of such eigenfunctions contains real exponentials in x, which by themselves would be unbounded in the opposite limit (i.e., $x \to -\infty$ versus $x \to \infty$ and vice versa). Moreover, these exponential contributions are also growing in time, since their time dependence is given by the linear dispersion relation (modulo the usual rescaling $k \mapsto 2k$ between the linear and the nonlinear PDEs [6]). The IST, however, provides a built-in mechanism to regularize these terms and produce a bounded solution. The most familiar result of such a balance between growing exponentials is, of course, the sech-shaped one-soliton solution of the Korteweg–deVries (KdV) equation, or that of the focusing NLS equation, but the mechanism is, of course, more general and applies with any IC.

The situation is similar for the focusing NLS with NZBC, except that in this case the above picture is only part of the story. This is because the continuous spectrum includes a portion of the imaginary axis of the spectral parameter. As we saw in section 6, in the small-deviation limit, the contribution from the Jost eigenfunctions on the branch cut coincides exactly with that of the unstable Fourier modes.

Thus, the machinery of the IST encompasses both the linear and the nonlinear stage of the MI. In the linear stage, when the deviations from the constant background are small, the IST reproduces the results of the linearized NLS equation (modulo the contributions of the discrete eigenvalues if any are present), namely, exponentially growing Fourier modes. Unlike the linearization, however, the IST has a natural

mechanism for the saturation of such growing modes (via the combination of exponential terms in the solution of the inverse problem), in a manner similar to that of the automatic saturation and stabilization of the growing exponentials in the soliton solutions.

It should be noted that the exponential growth/decay of the Jost eigenfunctions in our formulation of the IST is just a choice of normalizations (made here as in [23] so that the Jost eigenfunctions are simultaneous solutions of both parts of the Lax pair), which is in direct correspondence with the fact that the scattering coefficients are constant in time in this framework. Alternatively, in the standard approach to IST [6, 40, 41] one imposes fixed boundary conditions for the Jost eigenfunctions, but then the Jost eigenfunctions are not solutions of the second half of the Lax pair, and the reflection coefficients become dependent on time. In particular, for the focusing NLS equation with NZBC, the reflection coefficients evaluated in the branch cut will grow/decay exponentially in the standard approach. The two approaches are obviously equivalent since they yield exactly the same expression for the reconstruction formula. Moreover, with either approach the simultaneous eigenfunctions of both parts of the Lax pair corresponding to values of k in the branch cut grow/decay exponentially in time. (Again, this is similar to what happens for Maxwell–Bloch systems [1, 25, 26, 27, 31, 48].) And, of course, the instability of the Fourier modes corresponding to eigenfunctions evaluated on the branch cut is not an artifact, but is instead a real feature of the PDE.

Of course, if one or more discrete eigenvalues are present, their contribution to the solution has no counterpart in the linearization. Therefore, *even for small-deviation IC, in general the IST provides a more accurate description of the dynamics than the linearization of the NLS equation.* In any case, however, we reiterate that the solitons *cannot* be the main vehicle for the MI, since there exists a class of perturbations of the constant background for which no discrete spectrum is present (e.g., potential wells with small phase difference; see section 5).

The results of this work suggest a number of questions. Regarding the discrete spectrum of the scattering problem, an interesting question is whether the characterization in section 5 regarding the number and location of discrete eigenvalues can be generalized to a broader class of IC. For box-like IC, there is at most one discrete eigenvalue as $\varepsilon \to 0$. One question is whether this remains true for generic potentials. Another interesting question is whether one can formulate upper bounds on the number of discrete eigenvalues in terms of appropriate moments of the potential. (These kinds of bounds are known for the KdV equation [6, 17], but no such results are possible for the NLS equation with ZBC [19].) Generally speaking, one could expect that potentials which are "close" (in some appropriate functional space) to the class considered here would have a correspondingly similar spectrum. On the other hand, for the focusing NLS equation this might not always be the case [19].

With regard to MI, a precise characterization of its nonlinear stage remains a key open question—even for the simple IC considered in this work. More specifically, an important task will be to obtain precise estimates for the maximum (i.e., saturated) amplitude of the Fourier coefficients associated with the linearly unstable modes. The IST makes it possible to do so for the first time in more than 40 years. Indeed, we expect that it will be possible to perform such a calculation by evaluating the long-time asymptotic behavior of the solutions using the Deift–Zhou method [18, 20]. Another important issue will also be to compare the instability mechanism for the case of NZBC to that for the case of periodic boundary conditions, to see whether they

are the same or different. It is well known that, for the focusing NLS equation with periodic boundary conditions, nontrivial homoclinic solutions exist which can lead to effective chaos [3, 4, 14, 39]. But MI is a different phenomenon. On one hand, it is unclear what is the analogue of the homoclinic solutions in the problem on the infinite line. If the homoclinic solutions are the analogue of the solitons of the infinite line, then either they are not the primary mechanism responsible for the MI, or the mechanism is different in the periodic case versus the infinite line case, since we have seen that, generically speaking, in the latter case MI is mediated by a portion of the continuous spectrum. Note also that with periodic boundary conditions, a threshold exists for MI: constant backgrounds with amplitudes below such a threshold are linearly stable. On the other hand, no threshold for instability exists for the NLS on the infinite line with NZBC. The difficulty in establishing a precise comparison between the periodic case and the infinite line is compounded by the fact that, to this day, there is no formulation of the IST with periodic boundary conditions that allows one to take the limit of the period to infinity in a convenient way. It is hoped that these and other open questions can be addressed in the future.

Appendix A. Notation and symmetries. Throughout this work, complex conjugation is denoted by an asterisk, and matrix transpose by the superscript T. The set of nonnegative integers is $\mathbb{N}_0 = \{0, 1, 2, \dots\}$. The Pauli matrices,

$$\sigma_1 = \begin{pmatrix} 0 & 1 \\ 1 & 0 \end{pmatrix}, \qquad \sigma_2 = \begin{pmatrix} 0 & -i \\ i & 0 \end{pmatrix}, \qquad \sigma_3 = \begin{pmatrix} 1 & 0 \\ 0 & -1 \end{pmatrix}, \tag{A.1}$$

satisfy the relation $\sigma_j \sigma_k = \delta_{jk} I + i\epsilon_{jkl}\sigma_l$, where δ_{jk} is the Kronecker delta, I is the 2×2 identity matrix, and ϵ_{jkl} is the totally antisymmetric Levi–Civita tensor. The direct and inverse Fourier transform pair is defined as

$$\hat{f}(\zeta) = \mathcal{F}_\zeta[f] = \int_{\mathbb{R}} \mathrm{e}^{-i\zeta x} f(x)\,\mathrm{d}x\,, \quad f(x) = \mathcal{F}_x^{-1}[\hat{f}] = \frac{1}{2\pi}\int_{\mathbb{R}} \mathrm{e}^{i\zeta x}\hat{f}(\zeta)\,\mathrm{d}\zeta\,. \tag{A.2}$$

The proofs of Theorems 5.1 and 5.4 use the following formulation of Rouché's theorem (e.g., see [15, 37]), which does not require analyticity on the boundary of the domain.

THEOREM *(Rouché's theorem). If the two functions $f(z)$ and $g(z)$ are analytic in an open, connected set D and if $|f(\xi)| < |g(\xi)|$ holds at every point ξ of the boundary of D, the two functions $g(z)$ and $f(z) + g(z)$ have the same number of zeros in D.*

Next we obtain various symmetries of the eigenfunctions and scattering data. These are well known in the case of ZBC, but their analogues in the case of NZBC are not, since the IST for that case is more recent. Recall that if $q(x,t)$ is any solution of the NLS equation and α, x_o, and t_o are any real constants, $\bar{q}(x,t) = \mathrm{e}^{i\alpha} q(x,t)$ and $\check{q}(x,t) = q(x - x_o, t - t_o)$ are also solutions of the NLS equation. We next show how each of these transformations affects the IST.

LEMMA A.1. *Let $\bar{\phi}_\pm(x,t,z)$ and $\bar{S}(z)$ be the Jost solutions and scattering matrix corresponding to $\bar{q}(x,t)$. We have*

$$\bar{\phi}_\pm(x,t,z) = \mathrm{e}^{i(\alpha/2)\sigma_3}\phi_\pm(x,t,z)\mathrm{e}^{-i(\alpha/2)\sigma_3}, \quad \bar{S}(z) = \mathrm{e}^{i(\alpha/2)\sigma_3} S(z)\mathrm{e}^{-i(\alpha/2)\sigma_3}. \tag{A.3}$$

Proof. We have $\bar{Q}(x,t) = \mathrm{e}^{i(\alpha/2)\sigma_3} Q(x,t)\mathrm{e}^{-i(\alpha/2)\sigma_3}$, which implies that $\bar{E}_\pm(z) = \mathrm{e}^{i(\alpha/2)\sigma_3} E_\pm(z)\mathrm{e}^{-i(\alpha/2)\sigma_3}$. Then $\mathrm{e}^{i(\alpha/2)\sigma_3}\phi_\pm(x,t,z)$ and $\bar{\phi}_\pm(x,t,z)$ are both fundamental matrix solutions of the asymptotic scattering problem, and as a result there exists

an invertible 2×2 matrix $C(z)$ such that $\bar{\phi}_\pm(x,t,z) = \mathrm{e}^{-i(\alpha/2)\sigma_3}\phi_\pm(x,t,z)C(z)$. Comparing the asymptotics as $x \to \pm\infty$ yields the first equation of (A.3). Then, recalling that $\bar{\phi}_+(x,t,z) = \bar{\phi}_-(x,t,z)\bar{S}(z)$ yields the second equation of (A.3). ∎

LEMMA A.2. *Let $\check{\phi}_\pm(x,t,z)$ and $\check{S}(z)$ be the Jost solutions and scattering matrix corresponding to $\check{q}(x,t)$. We have*

(A.4)
$$\check{\phi}_\pm(x,t,z) = \phi_\pm(x,t,z)\mathrm{e}^{i\theta(x_o,t_o,z)\sigma_3}, \quad \check{S}(z) = \mathrm{e}^{-i\theta(x_o,t_o,z)\sigma_3}S(z)\mathrm{e}^{i\theta(x_o,t_o,z)\sigma_3}.$$

The proof of Lemma A.2 is omitted since it is similar to that of Lemma A.1.

Finally, we note that the NLS equation also possesses a Galilean invariance; i.e., if $q(x,t)$ is a solution, so is $q_v(x,t) = \mathrm{e}^{iv(x-vt)}q(x-2vt,t)$. Note, however, that if $q(x,t)$ does not vanish as $x \to \pm\infty$, then $q_v(x,t)$ is outside the class of potentials for which the IST formalism developed in [12] can be applied. Therefore, no simple correspondence between the Jost solutions and scattering matrices can be established.

Appendix B. Even potentials with NZBC. Next we obtain the symmetries possessed by the scattering data when the potential is an even function of x. First recall that the NLS equation possesses the following phase and scaling invariances: if $q(x,t)$ satisfies the NLS equation, then so do $\mathrm{e}^{i\alpha}q(x,t)$ and $aq(ax,a^2t)$ for arbitrary real α and a. Thus, we may assume without loss of generality that $q_- = q_o = 1$.

Also recall that the NLS equation is invariant under space reflections: if $q(x,t)$ satisfies the NLS equation, so does $q(-x,t)$. Let $\tilde{Q}(x,t) = Q(-x,t)$, and suppose that $\phi_\pm(x,t,k)$ satisfy both the Lax pair (2.3) and the asymptotic conditions (2.6). Let us derive the symmetries of the eigenfunctions and scattering data under the transformation $Q(x,t) \mapsto \tilde{Q}(x,t)$. Since the scattering coefficients are independent of time, we derive their relations at $t=0$. Since $\tilde{Q}_\pm = Q_\mp$ and $\lambda(-k) = -\lambda(k)$, we have that $w(x,t,k) = \sigma_3\phi_\mp(-x,t,-k)\sigma_3$ solves the Lax pair with $Q(x,t)$ replaced by $\tilde{Q}(x,t)$ and satisfies the asymptotic condition (2.6) with $Q_\pm$ replaced by $\tilde{Q}_\pm$. Thus, $w(x,t,k) = \tilde{\phi}_\pm(x,t,k)$, implying

$$\tilde{\phi}_\pm(x,t,k) = \sigma_3\phi_\mp(-x,t,-k)\sigma_3\,. \tag{B.1}$$

As a consequence, the new scattering matrix is given by

$$\tilde{S}(k) = \sigma_3 S^{-1}(-k)\sigma_3\,.$$

In particular, $\tilde{s}_{1,1}(k) = s_{2,2}(-k)$. In the case of an even potential (i.e., $\tilde{Q}(x,t) = Q(x,t)$) we have $\tilde{\phi}_\pm(x,t,k) = \phi_\pm(x,t,k)$ and $\tilde{S}(k) = S(k)$, so $s_{1,1}(k) = s_{2,2}(-k) = s_{1,1}^*(-k^*)$. Thus, discrete eigenvalues appear in symmetric quartets, i.e., $\pm k_n, \pm k_n^*$, or, when formulated in the uniformization variable, in symmetric octets, as in the boundary value problem with ZBC [10, 11]. This allows us to confine our search for discrete eigenvalues to $\overline{\mathbb{C}}_{\mathrm{I}}$ in Theorems 5.1 and 5.4.

Symmetry relations also exist between the norming constants associated to symmetric eigenvalues. To derive them, it is convenient to use the uniformization variable $z = k + \lambda(k)$. Denote by $z_{n'} = -z_n^*$ the eigenvalue symmetric to z_n in the upper half-plane, and by $C_{n'}$ the associated norming constant, as in section 2. Substituting the symmetries (B.1) for the Jost eigenfunctions in (2.8), and using the generic symmetry $\tilde{b}_n = -b_n^*$, the norming constants satisfy the constraint

$$b_n b_{n'}^* = 1\,, \qquad C_n C_{n'}^* = -\frac{1}{\left(s_{1,1}'(z_n)\right)^2}\,, \tag{B.2}$$

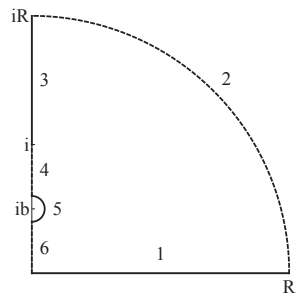

1. $k = x$, $0 \le x \le R$.
2. $k = R\mathrm{e}^{i\theta}$, $0 < \theta < \pi/2$.
3. $k = iy$, $1 < y \le R$.
4. $k = iy$, $b < y \le 1$.
5. $k = ib + \varepsilon \mathrm{e}^{i\theta}$, $-\pi/2 < \theta < \pi/2$.
6. $k = iy$, $0 < y < b$.

FIG. 6. *The contour C for Rouché's theorem for the potential well and the parametrizations for the corresponding six segments.*

where the relation $s'_{1,1}(z_{n'}) = -(s'_{1,1}(z_n))^*$ was used. These relations are formally identical to those for the norming constants of symmetric eigenvalues for even potentials with ZBC [11], except that in (B.2) the derivative of the analytic scattering coefficient is taken with respect to z instead of k.

Appendix C. Proofs. Here we prove the theorems and lemmas stated in section 5.

Proof of Theorem 5.1. Consider the region D bounded by the contour $C \subset \overline{\mathbb{C}}_{\mathrm{I}}$ composed of the six segments illustrated in Figure 6. With our choice of square root signs, $\lambda(k)$ is analytic on $\mathbb{C}_{\mathrm{I}}$ and continuous up to the boundary, including the limit to the branch cut from the right. We chose $\operatorname{Im}\mu(k) \ge 0$ on $\overline{\mathbb{C}}_{\mathrm{I}}$ (but $s_{1,1}(k)$ is independent of the choice). Using the $F(k)$, $G(k)$ defined in (4.8), we will show $|F(k)| < |G(k)|$ on C. Thus, $F(k) + G(k)$ and $G(k)$ have the same number of zeros in D. But we will also show $G(k) \ne 0$ in D. Thus, $s_{1,1}(k)$ has no zeros, i.e., no discrete eigenvalues in $\overline{\mathbb{C}}_{\mathrm{I}}$. The symmetries of the scattering coefficients allow us to conclude that there are no eigenvalues in the upper half-plane.

We first show that $G(k) \ne 0$ in D. A zero k of $G(k)$ must satisfy the equation $\lambda^2\mu^2 = (b\cos\alpha + k^2)^2$, which in turn implies

$$-k^2 = \frac{b^2(1-\cos^2\alpha)}{(1-b)^2 + 2b(1-\cos\alpha)}\,.$$

Both the numerator and denominator in the above expression are always nonnegative. Thus any solution must be purely imaginary and therefore does not lie in the interior of D.

We now turn to the comparison of $F(k)$ and $G(k)$ along C.

On segment 1, k, $\lambda(k)$, and $\mu(k)$ are real and nonnegative. Comparing the signs in (4.8) yields $|\tilde{F}(k)| < |\tilde{G}(k)|$ for k in segment 1. Since $|\mathrm{e}^{\pm 2iL\mu}| \equiv 1$ there, $|F(k)| < |G(k)|$.

On segment 2, as $R \to \infty$ we have $|\mathrm{e}^{-2iL\mu}| \to \infty$, $|\mathrm{e}^{2iL\mu}| \to 0$, and $\lambda\mu = k^2(1 + o(1))$, respectively. Thus, for large enough R we have $|F(k)| < |G(k)|$ for all k on segment 2.

On segment 3, $k = iy$ with $1 < y \le R$, so k, $\lambda(k)$, and $\mu(k)$ are all purely imaginary, but $\tilde{F}(k)$ and $\tilde{G}(k)$ are real. Also, $b\cos\alpha - y^2 < 0$ and $\lambda\mu < 0$, so $|\tilde{F}(k)| < |\tilde{G}(k)|$. Moreover, $\mathrm{e}^{2iL\mu} < \mathrm{e}^{-2iL\mu}$ on segment 3. Therefore $|F(k)| < |G(k)|$ there.

On segment 4, k and $\mu(k)$ are purely imaginary, and $\lambda(k)$ is real. As a result, we have $|\tilde{F}(k)| \equiv |\tilde{G}(k)|$ there. But $\mathrm{e}^{2iL\mu} < \mathrm{e}^{-2iL\mu}$, so again $|F(k)| < |G(k)|$.

Regarding segment 5, the hypotheses of Rouché's theorem do not hold at $k = ib$, where $F(k)+G(k) = 0$. As a consequence, we deform the contour away from $k = ib$ to an arbitrarily small neighborhood to the right of the branch point. For $k = ib + \varepsilon e^{i\theta}$, with $-\pi/2 < \theta < \pi/2$, we have the following for $\lambda(k)$ and $\mu(k)$:

$$\lambda(k) = \sqrt{1-b^2} + \frac{ib e^{i\theta}}{\sqrt{1-b^2}}\varepsilon + O(\varepsilon^2)\,,$$
$$\mu(k) = \sqrt{2b}\, e^{i(\theta/2+\pi/4)}\sqrt{\varepsilon} + \frac{e^{i(3\theta/2-\pi/4)}}{2\sqrt{2b}}\varepsilon^{3/2} + O(\varepsilon^{5/2})\,.$$

Since $|e^{2iL\mu}| < 1 < |e^{-2iL\mu}|$, we need only show $|\tilde{F}(k)| \le |\tilde{G}(k)|$. We may write

$$\tilde{F}(k) = f_o + f_1\sqrt{\varepsilon} + O(\varepsilon)\,, \qquad \tilde{G}(k) = g_o + g_1\sqrt{\varepsilon} + O(\varepsilon)\,,$$

where

$$f_o = -g_o = b(b-\cos\alpha)\,, \qquad f_1 = g_1 = (1+i)\sqrt{b(1-b^2)}e^{i\theta/2}\,.$$

Thus we have

$$\begin{aligned}|\tilde{G}(k)|^2 - |\tilde{F}(k)|^2 &= (|g_o|^2 - |f_o|^2) + 2(\mathrm{Re}(g_o g_1^*) - \mathrm{Re}(f_o f_1^*))\sqrt{\varepsilon} + O(\varepsilon)\\ &= 4\,\mathrm{Re}(g_o g_1^*)\sqrt{\varepsilon} + O(\varepsilon)\\ &= 4b(b-\cos\alpha)\sqrt{2b(1-b^2)}\,\cos\left(\frac{\theta}{2}+\frac{\pi}{4}\right)\sqrt{\varepsilon} + O(\varepsilon)\,.\end{aligned}$$

The $O(\sqrt{\varepsilon})$ term is positive for $-\pi/2 < \theta < \pi/2$. Thus, for all sufficiently small ε, we have the strict inequality $|F(k)| < |G(k)|$ on $k = ib + \varepsilon e^{i\theta}$.

On segment 6, $k = iy$ with $0 < y < b$, and $\lambda(k)$ and $\mu(k)$ are real and nonnegative. Here we use the fact that $\cos\alpha > b$, so $b\cos\alpha - y^2 > 0$, and again, $|F(k)| < |G(k)|$.

Taking R arbitrarily large and ε arbitrarily small, we conclude that $G(k)$ and $F(k)+G(k)$ have the same number of zeros in the first quadrant. We already showed that $G(k) \neq 0$ in the first quadrant, so $F(k)+G(k) \neq 0$ there. Thus, there can be no discrete eigenvalues in $\mathbb{C}_{\mathrm{I}}$ and, by the symmetries of the scattering coefficient, in the closure of the upper half-plane. ∎

Remarks. A few comments are in order. (i) As part of the proof, we have shown there are no purely imaginary discrete eigenvalues. (ii) If we had chosen the opposite sign for $\mu(k)$, the moduli of $F(k)$ and $G(k)$ would be switched, but we could have applied Rouché's theorem by switching their roles. (iii) Rouché's theorem cannot be applied when $\cos\alpha \le b$ with the same choice of $F(k)$ and $G(k)$, because the hypotheses are not satisfied along segment 6.

Proof of Theorem 5.2. We use the parametrization $k = iy$, with $1 < y < b$. Here, $\mu(k) = \sqrt{b^2-y^2}$ is a positive, strictly decreasing function of y from $\sqrt{b^2-1}$ to 0. Rewriting (4.6) and expressing k and λ in terms of μ, we obtain

$$\cot(2L\mu) = \frac{\mu^2 + b_\alpha^2 - b^2}{\mu\sqrt{b^2-1-\mu^2}}\,. \tag{C.1}$$

The denominator of the right-hand side of (C.1) is positive in $(0, \sqrt{b^2-1})$, but vanishes at the endpoints. The numerator is strictly increasing as a function of μ, and is negative at $\mu = 0$ and positive at $\mu = \sqrt{b^2-1}$. Thus, the right-hand side of (C.1)

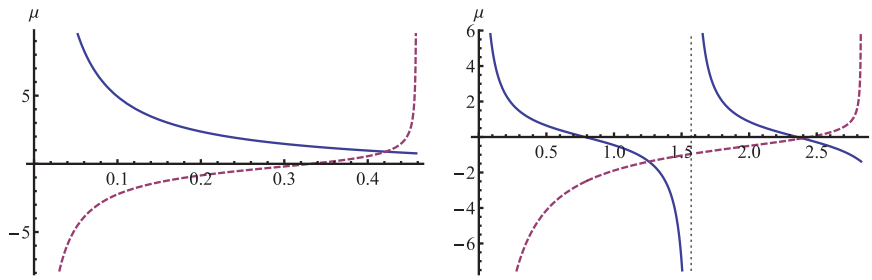

FIG. 7. *The left-hand side (thick solid curve, blue online) and right-hand side (thick dashed curve, purple online) of* (C.1) *as a function of* μ *for* $0 < \mu < \sqrt{b^2-1}$. *Left:* $b = 1.1$, $\alpha = 0$, *and* $L = 1$. *Right:* $b = 3$, $\alpha = \pi/8$, *and* $L = 1$. *In both cases,* $b_\alpha > 1$. *The discrete eigenvalues are given by the intersections of the two curves.*

tends to $-\infty$ as $\mu \to 0$ from the right; it tends to ∞ as $\mu \to \sqrt{b^2-1}$ from the left. By continuity it takes on all real values between these two limits. Moreover, one can show that its derivative is always positive. On the other hand, for each fixed L, the left-hand side of (C.1) tends to ∞ as $\mu \to 0^+$, and is locally a strictly decreasing function of μ wherever it is defined. If $L < \pi/(2\sqrt{b^2-1})$, there is exactly one intersection (see Figure 7 (left)). More generally, if $(n-1)\pi/(2\sqrt{b^2-1}) < L < n\pi/(2\sqrt{b^2-1})$, the graph of the left-hand side is composed of n strictly decreasing sections, so there are exactly n intersections (see Figure 7 (right)). $\square$

Proof of Theorem 5.4. We again look for the zeros of (4.5) by looking for values $k \notin i(1,b)$ such that (4.7) holds. We will use the decomposition (4.8) and Rouché's theorem, as in the proof of Theorem 5.1. However, we must now modify the contour, because for $k = iy$ with $1 \le y \le b$, we have $|F(k)| = |G(k)|$, so the hypotheses of Rouché's theorem are not satisfied there. Instead, we use the modified contour shown in Figure 8.

On segments 1–3 and 7, the arguments are analogous to those of Theorem 5.1. On segments 4, 5, and 6 we have $|\mathrm{e}^{2iL\mu}| < 1 < |\mathrm{e}^{-2iL\mu}|$, so it suffices to show $|\tilde{F}(k)| \le |\tilde{G}(k)|$.

On segment 4, $k(\varepsilon) = ib + \varepsilon \mathrm{e}^{i\theta}$, with $0 \le \theta < \pi/2$, implying

$$\lambda(k) = i\sqrt{b^2-1} + \frac{b\mathrm{e}^{i\theta}}{\sqrt{b^2-1}}\varepsilon + O(\varepsilon^2)\,,$$

$$\mu(k) = \sqrt{2b}\,\mathrm{e}^{i(\theta/2+\pi/4)}\sqrt{\varepsilon} + \frac{\mathrm{e}^{i(3\theta/2-\pi/4)}}{2\sqrt{2b}}\varepsilon^{3/2} + O(\varepsilon^{5/2})\,.$$

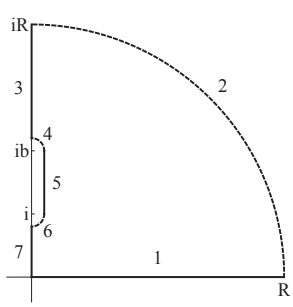

1. $k = x$, $0 \le x \le R$.
2. $k = R\mathrm{e}^{i\theta}$, $0 < \theta < \pi/2$.
3. $k = iy$, $b < y \le R$.
4. $k = ib + \varepsilon\mathrm{e}^{i\theta}$, $0 \le \theta < \pi/2$.
5. $k = \varepsilon + iy$, $1 < y < b$.
6. $k = i + \varepsilon\mathrm{e}^{i\theta}$, $-\pi/2 < \theta \le 0$.
7. $k = iy$, $0 < y < 1$.

FIG. 8. *The contour* C *for Rouché's theorem for the potential barrier and the corresponding segments.*

We may therefore expand $\tilde{F}(k)$ and $\tilde{G}(k)$ as

$$\tilde{F}(k) = f_o + f_1\sqrt{\varepsilon} + O(\varepsilon)\,, \qquad \tilde{G}(k) = g_o + g_1\sqrt{\varepsilon} + O(\varepsilon)\,,$$
$$f_o = -g_o = b(b-\cos\alpha)\,, \qquad f_1 = g_1 = (-1+i)\mathrm{e}^{i\theta/2}\sqrt{b(b^2-1)}\,.$$

Observing that f_o, g_o are real, we have

$$\begin{aligned}|\tilde{G}(k)|^2 - |\tilde{F}(k)|^2 &= 4g_o \operatorname{Re} g_1\sqrt{\varepsilon} + O(\varepsilon)\\ &= 4b(b-\cos\alpha)\sqrt{2b(b^2-1)}\,\sin\left(\frac{\theta}{2}+\frac{\pi}{4}\right)\sqrt{\varepsilon} + O(\varepsilon)\,.\end{aligned}$$

For $\theta \in [0,\pi/2)$ the $O(\sqrt{\varepsilon})$ term is positive. So for small enough ε, $|\tilde{G}(k)|^2 > |\tilde{F}(k)|^2$.

On segment 5, $k(\varepsilon) = \varepsilon + iy$, with $1 < y < b$, implying

$$\lambda(k) = i\sqrt{y^2-1} + \frac{y}{\sqrt{y^2-1}}\varepsilon + O(\varepsilon^2)\,,$$
$$\mu(k) = \sqrt{b^2-y^2} + \frac{iy}{\sqrt{b^2-y^2}}\varepsilon + O(\varepsilon^2)\,.$$

We then have

$$\tilde{F}(k) = f_o + f_1\varepsilon + O(\varepsilon^2)\,, \qquad \tilde{G}(k) = g_o + g_1\varepsilon + O(\varepsilon^2)\,,$$

where

$$f_o = -g_o^* = y^2 - b\cos\alpha + i\sqrt{(b^2-y^2)(y^2-1)}\,,$$
$$f_1 = g_1^* = \frac{y(b^2-2y^2+1)}{\sqrt{(b^2-y^2)(y^2-1)}} - 2iy\,.$$

Thus

$$\begin{aligned}|\tilde{G}(k)|^2 - |\tilde{F}(k)|^2 &= 4\operatorname{Re}(g_o g_1^*)\varepsilon + O(\varepsilon^2)\\ &= \frac{4y\big(b(b-\cos\alpha)(y^2-1) + (b\cos\alpha-1)(b^2-y^2)\big)}{\sqrt{(b^2-1)(y^2-1)}}\varepsilon + O(\varepsilon^2)\,.\end{aligned}$$

The coefficient of the $O(\varepsilon)$ term is positive. Thus for small enough ε, $|\tilde{G}(k)|^2 > |\tilde{F}(k)|^2$.

On segment 6, $k(\varepsilon) = i + \varepsilon\mathrm{e}^{i\theta}$, with $-\pi/2 < \theta \le 0$, implying

$$\lambda(k) = \sqrt{2}\mathrm{e}^{i(\theta/2+\pi/4)}\sqrt{\varepsilon} - \frac{i\mathrm{e}^{i(3\theta/2+\pi/4)}}{2\sqrt{2}}\varepsilon^{3/2} + O(\varepsilon^{5/2})\,,$$
$$\mu(k) = \sqrt{b^2-1} + \frac{i\mathrm{e}^{i\theta}}{\sqrt{b^2-1}}\varepsilon + O(\varepsilon^2)\,.$$

We have

$$\tilde{F}(k) = f_o + f_1\sqrt{\varepsilon} + O(\varepsilon)\,, \qquad \tilde{G}(k) = g_o + g_1\sqrt{\varepsilon} + O(\varepsilon)\,,$$
$$f_o = -g_o = 1 - b\cos\alpha\,, \qquad f_1 = g_1 = \mathrm{e}^{i\theta/2}(1+i)\sqrt{b^2-1}\,,$$

so that

$$|\tilde{G}(k)|^2 - |\tilde{F}(k)|^2 = 4g_o \operatorname{Re} g_1\sqrt{\varepsilon} + O(\varepsilon)$$
$$= 4(b\cos\alpha - 1)\sqrt{2(b^2-1)}\,\sin\left(\frac{\theta}{2}+\frac{\pi}{4}\right)\sqrt{\varepsilon} + O(\varepsilon)\,.$$

For $\theta \in (-\pi/2, 0]$ the $O(\sqrt{\varepsilon})$ term is positive. Thus for small enough ε, $|\tilde{G}(k)|^2 > |\tilde{F}(k)|^2$.

Combining the above estimates and letting $R \to \infty$ and $\varepsilon \to 0$ as before, we conclude that there are no discrete eigenvalues off the segment $i(1,b)$ of the imaginary axis. ∎

Proof of Theorem 5.5. The inequality $|F(k)| < |G(k)|$ remains true on segment 3 even when $\cos\alpha \le b$. Thus there can be no zeros of $s_{1,1}(k)$ for $k \in i(1,\infty)$. ∎

Proof of Lemma 5.6. On the continuous spectrum, k^2, $\lambda(k)$, and $\mu(k)$ are real, so the left-hand side of (4.6) is real, while the right is purely imaginary. Thus, in order to have a zero, both sides must be zero. Thus, we must have $b\cos\alpha + k^2 = 0$. If $\cos\alpha > 0$, this occurs at $k = i\sqrt{b\cos\alpha} = ib_\alpha$. If $\cos\alpha < 0$, this occurs at $k = \sqrt{-b\cos\alpha}$. In both cases, $\mu = \sqrt{b^2 - b_\alpha^2}$, so $L = (2n+1)\pi/(4\sqrt{b^2-b_\alpha^2})$. ∎

Proof of Lemma 5.7. Evaluate (4.6) at $k = iy$ and solve for L. ∎

Proof of Theorem 5.8. For fixed n, $\ell(y,n)$ is continuous on $(1,b)$. As $y \to b^-$, $\ell(y,0) \to \infty$. As $y \to 1^+$, we have the following possibilities:

1. If $\cos\alpha < 1/b$, then $\ell(y,0) \to \pi/(2\sqrt{b^2-1})$ as $y \to 1^+$.
2. If $\cos\alpha = 1/b$, then $\ell(y,0) \to \pi/(4\sqrt{b^2-1})$ as $y \to 1^+$.
3. If $\cos\alpha > 1/b$, then $\ell(y,0) \to 0$ as $y \to 1^+$.

Thus, if $\cos\alpha < 1/b$, the range of $\ell(y,0)$ contains $(\pi/(2\sqrt{b^2-1}),\infty)$, so for $L > \pi/(2\sqrt{b^2-1})$ the scattering problem has a discrete eigenvalue in $i(1,b)$. If $\cos\alpha = 1/b$, the range of $\ell(y,0)$ contains $(\pi/(4\sqrt{b^2-1}),\infty)$ so for $L > \pi/(4\sqrt{b^2-1})$ the scattering problem has a discrete eigenvalue in $i(1,b)$. Finally (as we saw before), if $\cos\alpha > 1/b$, the range of $\ell(y,0)$ is $(0,\infty)$, so there is a discrete eigenvalue for every $L > 0$. ∎

Acknowledgments. We thank Mark Ablowitz, Percy Deift, Gregor Kovacic, Peter Miller, Barbara Prinari, and Vladimir Zakharov for many insightful conversations.

REFERENCES

[1] M. J. Ablowitz, D. J. Kaup, and A. C. Newell, *Coherent pulse propagation: A dispersive irreversible phenomenon*, J. Math. Phys., 15 (1974), pp. 1852–1858.

[2] M. J. Ablowitz, D. J. Kaup, A. C. Newell, and H. Segur, *The inverse scattering transform—Fourier analysis for nonlinear problems*, Stud. Appl. Math., 53 (1974), pp. 249–315.

[3] M. J. Ablowitz and C. M. Schober, *Effective chaos in the nonlinear Schrödinger equation*, Contemp. Math., 172 (1994), pp. 253–268.

[4] M. J. Ablowitz, C. M. Schober, and B. M. Herbst, *Numerical chaos, roundoff errors and homoclinic manifolds*, Phys. Rev. Lett., 71 (1993), pp. 2683–2686.

[5] M. J. Ablowitz and H. Segur, *The inverse scattering transform: Semi-infinite interval*, J. Math. Phys., 16 (1975), pp. 1054–1056.

[6] M. J. Ablowitz and H. Segur, *Solitons and the Inverse Scattering Transform*, SIAM, Philadelphia, 1981.

[7] T. B. Benjamin, *Instability of periodic wavetrains in nonlinear dispersive systems*, Proc. R. Soc. Lond. Ser. A, 299 (1967), pp. 59–76.

[8] T. B. Benjamin and J. E. Feir, *The disintegration of wave trains on deep water*, J. Fluid Mech., 3 (1967), pp. 417–430.

[9] R. F. Bikbaev and V. O. Tarasov, *Initial-boundary value problem for the nonlinear Schrödinger equation*, J. Phys. A, 24 (1991), pp. 2507–2516.
[10] G. Biondini and A. Bui, *On the nonlinear Schrödinger equation on the half line with homogeneous Robin boundary conditions*, Stud. Appl. Math., 129 (2012), pp. 249–271.
[11] G. Biondini and G. Hwang, *Solitons, boundary value problems and a nonlinear method of images*, J. Phys. A, 42 (2009), 205207.
[12] G. Biondini and G. Kovacic, *Inverse scattering transform for the focusing nonlinear Schrödinger equation with nonzero boundary conditions*, J. Math. Phys., 55 (2014), 031506.
[13] G. Biondini and B. Prinari, *On the spectrum of the Dirac operator and the existence of discrete eigenvalues for the defocusing nonlinear Schrödinger equation*, Stud. Appl. Math., 132 (2014), pp. 138–159.
[14] A. R. Bishop, M. G. Forest, D. M. McLauglin, and E. A. Overman, *A quasiperiodic route to chaos in a near-integrable PDE*, Phys. D, 23 (1986), pp. 293–328.
[15] C. Caratheodory, *Theory of Functions of a Complex Variable*, Vols. 1–2, Chelsea, New York, 1954.
[16] B. Deconinck and K. Oliveras, *The instability of periodic surface gravity waves*, J. Fluid Mech., 675 (2011), pp. 141–167.
[17] P. Deift and E. Trubowitz, *Inverse scattering on the line*, Comm. Pure Appl. Math., 32 (1979), pp. 121–251.
[18] P. Deift, S. Venakides, and X. Zhou, *The collisionless shock region for the long-time behavior of solutions of the KdV equation*, Comm. Pure Appl. Math., 47 (1994), pp. 199–206.
[19] P. Deift and X. Zhou, *Direct and inverse scattering on the line with arbitrary singularities*, Comm. Pure Appl. Math., 44 (1991), pp. 485–533.
[20] P. Deift and X. Zhou, *A steepest descent method for oscillatory Riemann-Hilbert problems: Asymptotics for the mKdV equation*, Ann. of Math. (2), 137 (1993), pp. 295–368.
[21] L. D. Faddeev and L. A. Takhtajan, *Hamiltonian methods in the theory of solitons*, Springer-Verlag, Berlin, 1987.
[22] A. S. Fokas, *An initial-boundary value problem for the nonlinear Schrödinger equation*, Phys. D, 35 (1989), pp. 167–185.
[23] A. S. Fokas, *A Unified Approach to Boundary Value Problems*, SIAM, Philadelphia, 2008.
[24] M. G. Forest, C. G. Goedde, and A. Sinha, *Chaotic transport and integrable instabilities in a near-integrable, many-particle, Hamiltonian lattice*, Phys. D, 67 (1993), pp. 347–386.
[25] I. R. Gabitov, A. V. Mikhailov, and V. E. Zakharov, *Superfluorescence pulse shape*, JETP Lett., 37 (1983), pp. 279–282.
[26] I. R. Gabitov, A. V. Mikhailov, and V. E. Zakharov, *Non-linear theory of superfluorescence*, Sov. Phys. JETP, 59 (1984), pp. 703–709.
[27] I. R. Gabitov, V. E. Zakharov, and A. V. Mikhailov, *Maxwell-Bloch equation and the inverse scattering method*, Theoret. and Math. Phys., 63 (1985), pp. 328–343.
[28] P. D. Hislop and I. M. Sigal, *Introduction to Spectral Theory. With Applications to Schrödinger Operators*, Springer-Verlag, New York, 1996.
[29] E. Infeld and G. Rowlands, *Nonlinear Waves, Solitons and Chaos*, Cambridge University Press, Cambridge, UK, 1990.
[30] A. L. Islas and C. M. Schober, *Predicting rogue waves in random oceanic sea states*, Phys. Fluids, 17 (2005), 031701.
[31] D. J. Kaup, *Coherent pulse propagation: A comparison of the complete solution with the McCall-Hahn theory and others*, Phys. Rev. A, 16 (1977), pp. 704–719.
[32] I. T. Khabibullin, *Integrable initial-boundary value problems*, Teoret. Mat. Fiz., 86 (1991), pp. 43–52.
[33] B. Kibler, J. Fatome, C. Finot, G. Millot, F. Dias, G. Genty, N. Akhmediev, and J. M. Dudley, *The Peregrine soliton in nonlinear fibre optics*, Nat. Phys., 6 (2010), pp. 790–795.
[34] Y. Kivshar and G. Agrawal, *Optical Solitons: From Fibers to Photonic Crystals*, Academic Press, San Diego, 2003.
[35] M. Klaus and J. K. Shaw, *On the eigenvalues of the Zakharov–Shabat systems*, SIAM J. Math. Anal., 34 (2003), pp. 759–773.
[36] E. A. Kuznetsov, *Solitons in a parametrically unstable plasma*, Sov. Phys. Dokl., 22 (1977), pp. 507–508.
[37] S. Lang, *Complex Analysis*, Addison-Wesley, Reading, MA, 1977.
[38] Y-C. Ma, *The perturbed plane-wave solutions of the cubic Schrödinger equation*, Stud. Appl. Math., 60 (1979), pp. 43–58.
[39] D. W. McLaughlin and E. A. Overman II, *Whiskered tori for integrable PDE's: Chaotic behavior in near integrable PDE's*, in Surveys in Applied Mathematics, Vol. 1, Plenum, New York, 1995, pp. 83–203.
[40] A. C. Newell, *Solitons in Mathematics and Physics*, SIAM, Philadelphia, 1985.

[41] S. P. Novikov, S. V. Manakov, L. P. Pitaevskii, and V. E. Zakharov, *Theory of solitons: The inverse scattering method*, Plenum, New York, 1984.

[42] D. H. Peregrine, *Water waves, nonlinear Schrödinger equations and their solutions*, J. Austral. Math. Soc. Ser. B, 25 (1983), pp. 16–43.

[43] J. Satsuma and N. Yajima, *Initial value problems of one-dimensional self-modulation of nonlinear waves in dispersive media*, Progr. Theoret. Phys. Suppl. No., 55 (1974), pp. 284–306.

[44] M. Tajiri and Y. Watanabe, *Breather solutions to the focusing nonlinear Schrödinger equation*, Phys. Rev. E, 57 (1998), pp. 3510–3519.

[45] V. O. Tarasov, *The integrable initial-boundary value problem on a semiline: Nonlinear Schrödinger equation and sine-Gordon equation*, Inverse Problems, 7 (1991), pp. 435–449.

[46] S. Trillo and S. Wabnitz, *Dynamics of the nonlinear modulational instability in optical fibers*, Optim. Lett., 16 (1991), pp. 986–988.

[47] G. B. Whitham, *Linear and Nonlinear Waves*, Wiley-Interscience [John Wiley & Sons], New York, London, Sydney, 1974.

[48] S. M. Zakharov and E. M. Manykin, *The inverse scattering formalism in the theory of photon (light) echo*, Sov. Phys. JETP, 55 (1982), pp. 227–231.

[49] V. E. Zakharov and A. A. Gelash, *Nonlinear stage of modulation instability*, Phys. Rev. Lett., 111 (2013), 054101.

[50] V. E. Zakharov and L. A. Ostrovsky, *Modulational instability: The beginning*, Phys. D, 238 (2009), pp. 540–548.

[51] V. E. Zakharov and A. B. Shabat, *Exact theory of two-dimensional self-focusing and one-dimensional self-modulation of waves in nonlinear media*, Sov. Phys. JETP, 34 (1972), pp. 62–69.

[52] V. E. Zakharov and A. B. Shabat, *Interaction between solitons in a stable medium*, Sov. Phys. JETP, 37 (1973), pp. 823–828.